

# Interference Estimation and Automated Generation of Spatial Re-use Map for Wireless Mesh Networks

*by*

**Pradeep Gopaluni**



**DEPARTMENT OF COMPUTER SCIENCE & ENGINEERING**

**INDIAN INSTITUTE OF TECHNOLOGY, KANPUR**

**June 2008**

# Interference Estimation and Automated Generation of Spatial Re-use Map for Wireless Mesh Networks

*A Thesis Submitted*

**in Partial Fulfillment of the Requirements**

**for the Degree of**

**Master of Technology**

*by*

**Pradeep Gopaluni**



*to the*

**DEPARTMENT OF COMPUTER SCIENCE & ENGINEERING**

**INDIAN INSTITUTE OF TECHNOLOGY, KANPUR**

**June 2008**

# Certificate

This is to certify that the work contained in the thesis titled “*Interference Estimation and Automated Generation of Spatial Re-use Map for Wireless Mesh Networks*”, by *Pradeep Gopaluni*, has been carried out under my supervision and that this work has not been submitted elsewhere for a degree.

July, 2008

---

(Dr. Dheeraj Sanghi)

Department of Computer Science & Engineering,

Indian Institute of Technology, Kanpur

## Abstract

Inter-link interference is one of the major factors that affects the performance of Wireless Mesh Networks. An *interference map* indicates possible spatial reuse, which can help improve the throughput of a TDMA-based network by reusing the same time slot for different non-interfering links. It is also a key input in both channel assignment and routing algorithms for the TDMA-based networks.

In this work, we have first performed various controlled measurements to study interference in realistic outdoor settings and determine the relation between the RSSI and interference. Based on the observations, we have developed a three way classification strategy to classify link-pairs according to the interference values. The classification strategy also takes care of the inherent RSSI variability observed in outdoor wireless links. It uses the SIR values approximated from the individual RSSI measurements, requiring only  $O(N)$  broadcast measurements for a network with  $N$  nodes .

We have also developed an automated mechanism, which performs these measurements periodically and generates an interference map. The time period of the measurements and the duration of each measurement is determined by time-series analysis of 24/48hr long duration data. The work done is specific to outdoor TDMA-based networks.

# Contents

<b>1</b>	<b>Introduction</b>	<b>1</b>
1.1	FRACTEL . . . . .	1
1.2	Motivation and Problem Statement . . . . .	3
1.3	Thesis Contributions . . . . .	4
1.4	Interference Background (Understanding Interference) . . . . .	4
1.5	Thesis Outline . . . . .	6
<b>2</b>	<b>Related Work</b>	<b>8</b>
<b>3</b>	<b>Interference Estimation</b>	<b>11</b>
3.1	Long-duration measurement versus short-duration measurement . . . . .	12
3.2	Measurement Setup and Procedure . . . . .	14
3.2.1	Aim . . . . .	14
3.2.2	Measurement Setup . . . . .	14
3.2.3	Hardware Setup . . . . .	15
3.2.4	Software Setup . . . . .	16
3.2.5	Measurement Procedure . . . . .	17
3.3	Interference Estimation using Signal to Interference Ratio . . . . .	18
3.3.1	Signal to Interference Ratio (SIR) . . . . .	19
3.3.2	Estimation of Delivery probability using SIR . . . . .	19
3.3.3	Results and explanations . . . . .	20
3.4	Three-way Classification using 2.5th percentile and 97.5th percentile SIR values . . . . .	25
3.4.1	The three - way classification . . . . .	25
3.4.2	Results and Analysis . . . . .	26
3.5	Conclusions . . . . .	33
<b>4</b>	<b>Time - Period analysis</b>	<b>39</b>
4.1	Long Duration Experiments . . . . .	39
4.1.1	802.11 (WiFi) . . . . .	39
4.1.2	802.15.4 (Sensor Networks) . . . . .	40
4.2	Spectral Analysis . . . . .	42
4.3	T and t analysis . . . . .	45
4.3.1	T - Example . . . . .	45
4.3.2	t - Example . . . . .	46
4.3.3	Results and Conclusions . . . . .	46

<b>5</b>	<b>Putting It together: An Automated Interference mapping</b>	<b>50</b>
5.1	Introduction . . . . .	50
5.2	An automated measurement and spatial reuse map generation procedure	52
5.2.1	Active Measurement . . . . .	53
5.2.2	Interference Map Generation . . . . .	54
5.2.3	Broadcast Schedule Generation . . . . .	54
<b>6</b>	<b>Conclusion and Future work</b>	<b>55</b>
6.1	Conclusion . . . . .	55
6.2	Future Work . . . . .	56
	<b>Bibliography</b>	<b>57</b>

# List of Tables

3.1	RSSI error between successive distributions of long-duration data . . . . .	13
3.2	RSSI error behavior with time . . . . .	13
3.3	SIR Band for the steep region (Roofnet) : Source [5] . . . . .	27
3.4	Accuracy for three-way classification 1Mbps . . . . .	29
3.5	Accuracy for three-way classification 2Mbps . . . . .	30
3.6	Accuracy for three-way classification 5.5Mbps . . . . .	31
3.7	Accuracy for three-way classification 11Mbps . . . . .	32
4.1	Average error (in mod-difference terms) for various t values . . . . .	48
5.1	Interference Map . . . . .	52

# List of Figures

1.1	FRACTEL example [14]	2
1.2	Carrier - Sensing / non-destructive interference	6
1.3	Hidden -terminal / destructive sensing interference	6
3.1	RSSI error behavior with time	14
3.2	Measurement Setup	15
3.8	Predicted vs Measured Delivery Probability	22
3.9	Predicted vs Measured Delivery Probability	23
3.11	Three way classification of 1Mbps links	28
3.12	3-way classification for 2Mbps	30
3.13	3-way classification for 5.5Mbps	31
3.14	3-way classification for 11Mbps	32
3.3	Experiment Locations[Reference: Google earth images]	34
3.4	Average RSSI versus TxPower graph for S1-R1 Link, Location1	35
3.5	Flow of events at $R_1$ (measurement procedure)	36
3.6	SIR distribution computed using convolutions	37
3.7	SINR versus Delivery Probability measured during an emulator experiment. Source:Roofnet measurement study [5].	37
3.10	Successive RSSI distributions for same link	38
4.1	Spectral Plots for 802.11, Location 1, Position 2	43
4.2	Auto - Correlogram for 802.11 link at Location 1, Position 2	44
4.3	Average error (in mod-difference terms) for various t values	47



4.4	Average Error (in mod-difference terms) for various $T$ values per different locations	49
5.1	An example interference scenario . . . . .	51

# Chapter 1

## Introduction

### 1.1 FRACTEL

A Wireless mesh network(WMN) is a co-operative set of wireless nodes, organized to form a communication network. These nodes together form a mesh topology, where any node can reach any other node in the network either directly or through some other nodes that have additional forwarding capabilities and act as mesh routers. One or more nodes in the mesh network may act as a gateway to the backbone network such as Internet, cellular network or some other communication network. Any node that wishes to communicate outside the network, sends its packets to the gateway either directly or with the help of mesh routers forming a multi-hop wireless network. WMNs are termed to be 'flexible' and 'scalable' networks. Flexible because the links need not be planned and scalable because of the fact that its size may vary from small indoor settings to large community networks with links ranging upto to tens and hundreds of kilometers [1, 2] and hundreds of nodes.

802.11 based wireless mesh networks has recently emerged as cost-effective solution for providing last hop Internet access. Past few years have seen many deployments [1, 4, 2] of outdoor and community mesh networks. These networks differ from the traditional wireless LANs in many ways and pose many research problems relating to the routing, channel assignment and MAC schemes that needs to be specifically designed for these kinds of settings.

FRACTEL (wi-Fi based **R**ural **A**ccess **T**ELephony) [7] is an 802.11 based rural wireless mesh network, for providing cost-effective Internet connectivity to the Rural regions. It uses

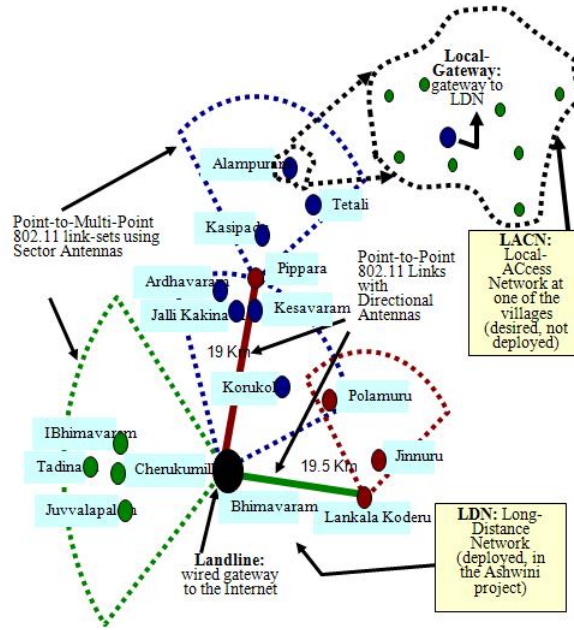


Figure 1.1: FRACTEL example [14]

off-the-shelf 802.11 hardware and a right combination of external antennas and tall towers to form a long distance wireless communication network. Because of the cheap availability of 802.11 hardware and relatively low establishment and maintenance costs of wireless links, these networks are efficient communication alternatives to their wired equivalent, especially when the user base is quite sparse like in rural settings.

FRACTEL network is a combination of long distance links and local access links. Long distance links connect wired back bone network to the central node in each village called local gateway. They also connect one local gateway to the other local gateways forming a multi-hop long distance network (LDN). These links are typically of tens of kilometers in length. Local gateway is then connected to several points (like schools and hospitals) in each village using what we call as “local access links”. These local access links are typically less than 500 meters. Each node in the village is connected to the local gateway by single-hop or through multiple hops of other village nodes. These nodes form a Local Access Network (LACN). Figure 1.1 depicts LDN and LACN in an example deployment setting in Ashwini network [14].

FRACTEL aims at providing voice and video capabilities for services like remote education and tele-medicine. It proposes the use of a TDMA based MAC designed specifically for providing these kind of services on long distance Wi-Fi links.

## 1.2 Motivation and Problem Statement

Wireless Mesh Networks are often unplanned and have dynamically changing links. The performance of these networks depends on effective management of these links. Inter-link interference is one of the key factors that affect the performance of wireless mesh networks. Many intelligent channel allocation and routing mechanisms try to work around the interference by operating the interfering links on separate orthogonal channels, and routing packets using separate non-interfering routes. The TDMA scheduling also tries to improve the throughput by spatially reusing the time slots by scheduling the non-interfering links on the same cycle. Thus, an *interference map* or *spatial re-use map* gives information relating to the inter-link interference, and the possibility of spatial reuse in a wireless mesh network.

There has been lot of work done to develop these intelligent routing and channel assignment schemes. Most of these schemes either assume that the required interference information is already present or use some pessimistic and inaccurate RF models to estimate the interference map. These RF-models like distance based path loss models and packet loss models which try to estimate the interference based on the RF - characteristics of a link are highly incapable of modeling the real world scenarios and cannot be used for generating the interference map. However, measuring interference is also non-trivial. An  $N$ -node network will have  $O(N^2)$  links and would require up to  $O(N^4)$  measurements to measure pair-wise interference. Owing to the fact that the wireless links exhibit some degree of RSSI variability, the interference measurement may not be a one time issue and adds to the complexity. Periodic repetition of the interference measurement also allows dynamic changes in the network and takes care of the inherent RSSI variability.

The main aim of this work is

- *To study interference characteristics, by careful and detailed experimentation*
- *To formulate an effective strategy for estimating interference based on actual measurements and*
- *To develop an automated mechanism to generate the spatial re-use map.*

The concept of interference map / spatial re-use map would be especially useful with medium

range networks, where the links are long enough to provide chances of spatial reuse, at the same time close enough to actually cause interference. So, the envisioned scenario for this automated mechanism is a LACN kind of setting FRACTEL network. The Long Distance Networks (LDN) on the other hand are permanent and can actually be planned out during establishment by using various combinations of directional antennas and tall towers [16].

### 1.3 Thesis Contributions

In this thesis we develop an automated mechanism for estimating inter-link interference in 802.11 based wireless mesh networks. We first perform several measurements, and study the interference characteristics in relation with already well established properties for out-door long distance links like variability and link abstraction. We then go on to propose an interference estimation and classification strategy.

#### **RSSI - based interference estimation**

The interference estimation scheme we present in this work is based on the premise that: there exists a strong correlation between the received signal strength at a particular receiver from two different senders and the amount of interference one exerts upon the other. This is called RSSI based interference estimation. The main advantage of RSSI based prediction is that it only requires us to measure the RSSI of each node at every other node. This can be measured, by each node broadcasting to every other node resulting in just  $O(N)$  measurements for  $N$  node network.

So, in this work we study this RSSI vs interference relation in detail, and devise an interference estimation strategy based on it. Finally we analyze the wireless data over long durations, to determine how the RSSI variability of the wireless links effects the measurement strategy. We use this to develop an automated mechanism to generate the spatial re-use map.

### 1.4 Interference Background (Understanding Interference)

In this section, we describe the basics of wireless interference, and see how it affects the link performance. The interfere in wireless networks can occur in several ways. It can be broadly

divided as

1. External interference and
2. Internal interference

External interference is the kind of interference whose source is outside our own network. It can either be a non-wireless source ( like a micro-wave device that operates on same frequency) or any other node from a different wireless network. External interference is not in our control. Internal interference on the other hand is caused by nodes from the same network. This kind of interference can be controlled, and hence the need to study. This interference among the links of same network is also called inter-link interference. Inter-link interference, when properly gaged can be avoided or controlled using separate channel assignments and alternate route formulations.

A wireless link may experience performance degradation due to the presence of interference either at the sender side or at the receiver side. At the sender, if the interferer signal power is above the sensitivity of the radio or its carrier sensing threshold, it causes the sender to back-off while carrier sensing causing delays. Here the packet is not actually lost but delayed from transmission causing performance degradation. This kind of interference is called carrier sensing interference or non-destructive interference. Figure 1.2 depicts the carrier sensing interference. The Figure shows two links  $S_1R_1$  and  $S_2R_2$ . The carrier sensing interference is caused if the received signal strength of the  $S_2$ 's transmission to  $R_2$  at  $S_1$  ( $RSSI_{S_2R_2}^{S_1}$ ) is above the carrier-sensing threshold.

$$RSSI_{S_2R_2}^{S_1} > \text{Carrier-Sensing threshold}$$

This particular relation is not symmetric. That is,  $S_1$  carrier sensing  $S_2$  does not mean that the reverse ( $S_2$  carrier sensing  $S_1$ ) is true. Non-destructive kind of interference is seen only in CSMA networks and will not be studied in this work.

Similarly at the receiver, the packet reception depends on the difference between the RSSI of sender and the interferer signal. Capture effect states that a packet is received if and only if the sender RSSI exceeds the interferer RSSI by a particular capture threshold. Otherwise, the packets would be lost due to collisions during reception. This kind of interference is called

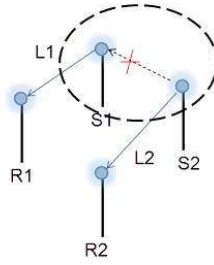


Figure 1.2: Carrier - Sensing / non-destructive interference

hidden terminal interference or destructive interference. Figure 1.3 shows two links  $S_1R_1$  and  $S_2R_2$ . Destructive interference occurs if and only if the signal strength of  $S_1$ 's transmission to  $R_1$  at  $R_1$  ( $RSSI_{S_1R_1}^{R_1}$ ) does not exceed the signal strength of  $S_2$ 's transmission to  $R_2$  at  $R_1$  ( $RSSI_{S_2R_2}^{R_1}$ ) by a certain capture threshold.

$$RSSI_{S_1R_1}^{R_1} - RSSI_{S_2R_2}^{R_1} < \text{capture-threshold}.$$

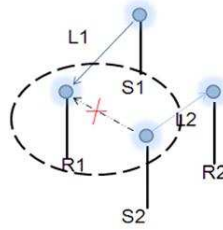


Figure 1.3: Hidden -terminal / destructive sensing interference

## 1.5 Thesis Outline

The thesis is organized as follows. In chapter 2, we present some of the work that has been done towards the interference estimation. Chapter 3 presents the interference estimation strategy we developed in this work. We first describe various measurements we performed during this work. We then develop an signal-to-interference ratio (SIR) based interference estimation strategy and evaluate it. We then use these results to propose a 3-way classification strategy for inter-link interference based on RSSI measurements.

In Chapter 4, we do time series analysis of long duration data for both 802.11 and 802.15.4 links. We use this data to calculate measurement duration and measurement interval for

creating an automated interference measurement strategy. In Chapter 6, we put all the results together to design and implement an automated mechanism to generate spatial reuse map.



## Chapter 2

# Related Work

In this chapter we will discuss some of the important work in this area. Interference information is key to many channel assignment and routing schemes. Most of the work on routing and channel assignment has also studied interference and proposed different heuristics like distance-based metrics for estimating interference. However [10] is the foremost work which showed that a measurement based approach is more accurate than using heuristics in a real network. Recent times has seen a lot of measurement based approaches [12, 6, 9] to accurately measure or estimate interference. There has also been work [15, 13] done to study various interference properties. We now discuss some of these works in detail and explain their take-aways and short comings.

### **Interference properties**

One of the important interference properties to study is the effect of multiple interferers on a single link. This is called multi-way interference. The works in [15, 13] have tried to study this aspect. The question [15] has tried to answer is, weather a combination of non-interfering nodes act together to cause interference. They have observed the effect of multi-way interference on a 32 node mesh network. To test it, first they isolated non interfering nodes and then used them simultaneously to measure the multi-way interference. While they conclude that the multi-way interference does exist, they say that it is not wide spread and recommend pair-wise measurements.

The work in [13] on the other hand studies the effect combination of two or more interfering

nodes. It proposes that the interfering nodes act independently and the delivery probability in presence of multiple interferers is the product of delivery probabilities when they act alone. That is, interference measurements for isolated triplets of nodes (sender - receiver - interferer) can be used to predict the damage from several simultaneous interferers. They experimentally verified this using their analytical model, and measurements in a controlled setting with three nodes. [10, 13] also study the correlation of interference with distance, and conclude that there is not much correlation and is a pessimistic way of estimating interference.

### Interference Measurements

One of the most significant work in the area of interference measurements is done in [10]. They propose a complete-measurement based approach for getting interference information. They develop a broadcast interference measurement scheme which tries to measure the pairwise interference in  $O(N^2)$  measurements, where  $N$  is the number of links. The paper uses broadcast messages instead of uni cast. It defines a metric broadcast interference ratio (BIR) as the ratio of broadcast good-put of two links operating separately versus the good put when they operate simultaneously. They have tested their metric in an indoor testbed and the measured BIR matches with the actual link interference ratio in most of the cases. Though the complexity of measurement is still very high, this work has shown that measurement based models are much more accurate than the heuristic based approaches, and also that the broadcast messages can be used to reduce the complexity for measuring interference.

The work in [6] on the other hand proposes a measurement based approach to model the delivery probability and interference in wireless networks. They propose probabilistic models for physical layer behavior of packet reception and carrier sensing in the presence interference. They use  $O(N)$  measurements to predict interference using their model. [9] also tries to model interference using measurements, they propose methodology that estimates the carrier sensing as well as the hidden terminal interference based on the RSSI measured. They propose a linear model to predict the amount of carrier sensing and amount of interference caused in relation to the RSSI and thus predict the good-put of the system. One of the take-aways here is that both the works use RSSI and  $O(N)$  measurements to create an interference estimation model, and show that there is a degree of correlation between RSSI and interference. But important

shortcomings are that they device and evaluate their work for an entirely different indoor setting and lack of experiment detail. They also fall short in explaining why such a relation (linear or probabilistic) exists.

Our approach differs with their work in the sense that we want to estimate interference in TDMA based networks, and does not consider carrier sensing interference. We want to study the interference specific to out-door long distance setting. We also want to device a strategy that takes into account the inherent variability of RSSI.

## Chapter 3

# Interference Estimation

In this chapter, we develop interference estimation strategy specific to TDMA-based networks like the FRACTEL [7] network. TDMA-based networks, unlike the traditional WiFi, are free of carrier sensing. However, disabling the carrier sensing for interference measurements using off-the-shelf WiFi hardware and drivers is non-trivial. Therefore, we work around this problem by using the concept of *hidden terminal*. A hidden node is defined as a node which cannot be carrier-sensed at the sender but causes interference at the receiver. As TDMA-based networks have no carrier-sensing, any node that causes interference is analogous to a hidden node. Therefore, to characterize and estimate inter-link interference in TDMA-based networks, we explicitly create hidden terminal cases and perform various measurements. We analyze this data to formulate a method of estimating the interference and generate an interference map.

In Section 3.1 we will analyse the long duration data to determine the merits of using the repeated short duration measurements instead of a single long duration measurement. The Section 3.2 describes the measurement setup, hardware and software details, and also the measurement procedure we have followed. In Section 3.3, we propose an interference estimation strategy and evaluate it. We then go on with classification of link-pairs based on interference in Section 3.4

### 3.1 Long-duration measurement versus short-duration measurement

In this section we try to answer one of the key questions in interference measurements - Is it possible to gauge the characteristics of a wireless link by a single long duration measurement, or should it be periodic short duration measurement. For this purpose, we take long duration data available from the FRACTEL measurement studies[8]. The data is collected continuously for 48/24hr duration over medium distance wireless links in six different positions. During these experiments the transmitter sends packets at an inter packet interval of 20 milliseconds and at full rate (11Mbps). The data is collected over two separate locations, with receiver at three different positions in each of the location. The following is the brief description of locations taken from [8]. Refer to FRACTEL measurement study for further details of the measurements.

- Location 1 (ACES Type II) : This location consists of several rows of two-storeyed houses on campus. There are a number of trees in the vicinity of the houses that are much taller than the house. Three separate 48hr duration experiments are conducted in this location. Let us call these locations - pos-1, pos-2 and pos-3.
- Location 2 (SBRA) :This location is the student residence; it has four rows of three-storeyed tall buildings along with few very short trees in the vicinity. Three 24hr experiments are conducted in this location. We call these locations - SBRA position 1, SBRA position 2 and SBRA position 3

Our aim in this analysis is to see if measuring RSSI for long duration, captures the link behavior correctly for a sufficiently large time period. This is a pre-requisite for settling down for a shorter duration experiment. For this we have first divided the 24hr data into two sets of 12hrs each (longest possible), and 48hr data into two sets of 24hr each. We then measured the error in RSSI distribution of the two sets. As a metric of accuracy to compare the two distributions we simply compute the area between them in the same graph (in 1dB units). This area can vary from zero, for similar distributions to a maximum of two. This is because the area under a given PDF curve is one, by definition.

<i>Position</i>	<i>Area</i>
SBRA pos1	0.352389
SBRA pos2	0.284252
SBRA pos3	0.702097
pos1	0.579739
pos2	0.258646
pos3	0.464925

Table 3.1: RSSI error between successive distributions of long-duration data

The Table 3.1 shows that the error is not close to zero, and proves that even by performing measurement for long-durations we will not be able to gauge the RSSI distribution, and hence interference accurately. Now, to see how this error behaves along with time in long-duration measurements, we split the long duration data further into windows of six hours each and computed the error (difference in area between the distribution) from the first six hours, to the successive six-hour windows.

	<b>6-12</b>	<b>12-18</b>	<b>18-24</b>	<b>24-30</b>	<b>30-36</b>	<b>36-42</b>	<b>42-48</b>
<b>SBRA pos1</b>	0.306541	0.270698	0.388895				
<b>SBRA pos2</b>	0.609841	0.792881	0.508670				
<b>SBRA pos3</b>	0.539836	1.076893	0.818174				
<b>pos1</b>	0.638391	0.708593	0.438357	0.822775	1.085188	1.038068	0.890730
<b>pos2</b>	0.461779	1.098385	0.393566	0.314516	0.773479	1.580660	0.454718
<b>pos3</b>	0.190493	0.501838	0.846101	0.573789	0.303887	1.168977	0.943512

Table 3.2: RSSI error behavior with time

From Figure 3.1 and Table 3.2, we can conclude the following.

1. The error (the area) is as high as 1.6, and consistently near one, which suggests that the amount of correlation is quite less for interference prediction.
2. The distribution of error, in terms of area is not following any pattern.

Thus we are unable to capture the link information completely even if we measure for longer duration continuously, hence we now proceed to develop an interference measurement strategy based on the short duration RSSI measurements in following sections

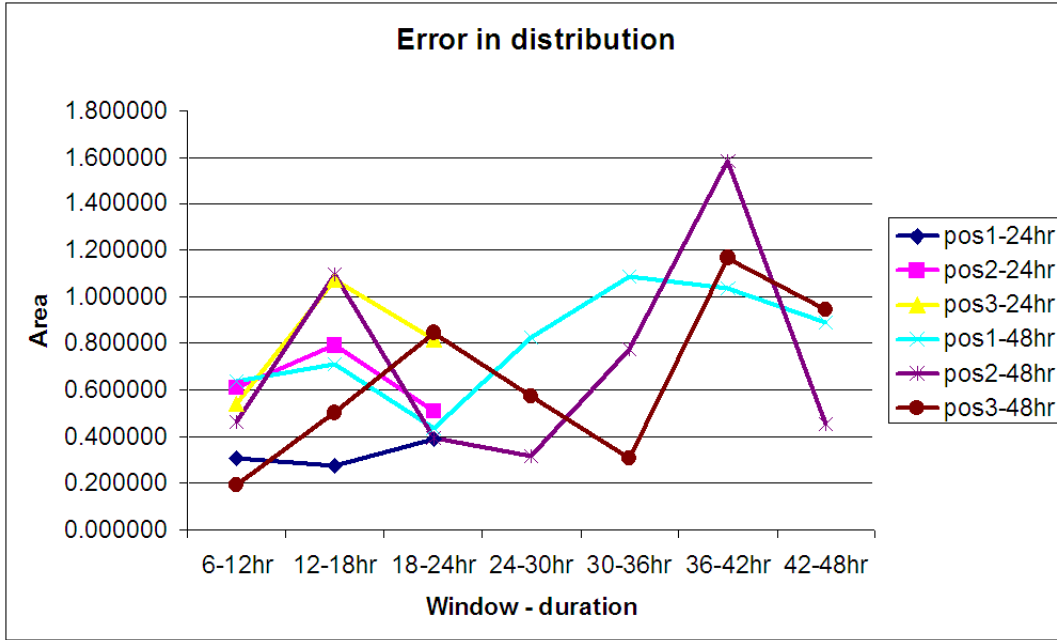


Figure 3.1: RSSI error behavior with time

## 3.2 Measurement Setup and Procedure

### 3.2.1 Aim

The aim of our measurements is to gauge the effect of the interferer signal strength on the amount of packet error rate observed. The measurements we perform, should help us in estimating the interference in out-door TDMA-based mesh networks like FRACTEL. Therefore, using these measurements, we want to see if we can “measure” the level of interference in realistic outdoor mesh settings instead of a controlled setting.

### 3.2.2 Measurement Setup

The measurement setup consists of three nodes: the sender  $S_1$ , the receiver  $R_1$  and the interferer  $S_2$ . The three nodes are placed such that the interferer  $S_2$  is hidden from the sender  $S_1$ , whereas the receiver  $R_1$  is in the range of both  $S_1$  and  $S_2$ . Since the transmit power assignment is not in the scope of this work, the intended destination of  $S_2$ 's transmission is irrelevant, and therefore, a fourth node is not required. This will create a couple of links  $S_1R_1$  and an imaginary  $S_2R_2$  (as  $R_2$  is not present) forming a link pair. The link  $S_2R_1$  here is the

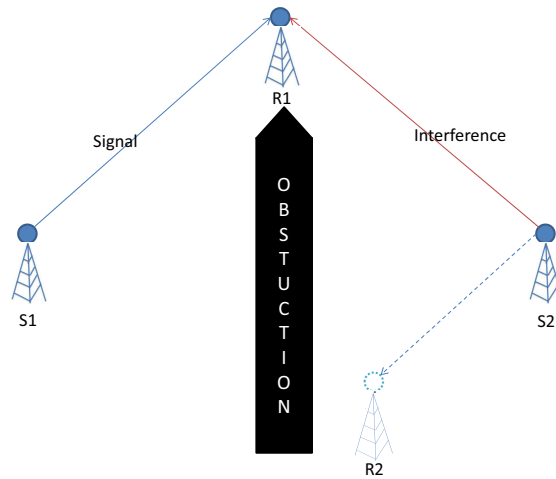


Figure 3.2: Measurement Setup

unintended link that acts as the interference as far as  $S_1R_1$  is concerned. Figure 3.2 gives the general idea of measurement setup.

### 3.2.3 Hardware Setup

For measurements, we used Ubiquity SuperRange2, 2.4 GHz, Mini-PCI Radios with Atheros chip set. These cards are fitted into SOEKRIS net4826, low-power, low-cost single board computers. Each of the nodes is connected to a external 8-dBi Omni directional antenna with the help of an RF-cable. The nodes are placed atop various buildings, and are powered up using batteries.

We have performed our experiments on two separate locations, which are chosen such that the sender and interferer has no line of sight, and are separated by huge buildings to avoid any carrier sensing. The following are the two experimental locations, where the measurements are conducted.

- **Location1 (Hostel 12, IITB):** In this setting the three nodes are placed on the terrace of the hostel building as shown in Figure 3.3a. The distance between the sender node and the receiver node is about 75m. And the distance between the interferer and the receiver node is 35m. The sender and the interferer are separated by huge building. There were no packets received at the sender when only interferer is transmitting and



vice-versa, thus creating a hidden node scenario. Both, sender and interferer have direct line of sight with the receiver. The location has no foliage. There are huge buildings on one side that cause multi-path. There is some external interference, but of negligible signal strength which is of order -93dBm and lower compared to the signal strength of the sender and the interferer which is about -65 to -85 dBm. The location is free of any kind external movement.

- **Location2 (Main building – GG building – KReSIT):** In this location, the distance between sender and receiver node is about 130mts and distance between interferer and receiver is 150 meters. Both, sender and interferer have direct line of sight with the receiver. Interferer is placed on top of KReSIT building, IITB and has external interference. The interferer-receiver link has clear line of sight and some foliage (tall trees) around (though not in line of sight) causing some degree of variable multipath. Sender is on 4th floor corridor of main building, IITB. There is a huge tree on the side of the node but clear from the line of sight. There is no external interference but there is small amount of carrier sensing of interferer at sender for max transmit power and 11b. Receiver node is kept on GG building, IITB. There is some interference from WiFi nodes within the KReSIT building. Buildings and foliage separate the interferer and the sender. The signal strength of both the links vary from -65dBm to -85dBm.

### 3.2.4 Software Setup

Multiband Atheros Driver for WiFi (MADWiFi) version 0.9.3 is used as the driver. We modified the driver to get the MAC header details along with the per-packet RSSI and Noise levels. These details are written onto a buffer in */proc*-file system by the driver. They are continuously read-out from */proc* and logged using a C-program. These logs are later analyzed using Ruby or Perl scripts.

The nodes communicate in Ad-Hoc demo (AHDEMO) mode provided by MADWiFi for exchange of parameters. AHDEMO mode is a pseudo-IBSS mode without beacons and associations. This will help avoid unnecessary packets in measurements. Once the interference

measurement starts, the receiver is changed to monitor mode while the other two nodes are kept in AHDEMO mode for transmission.

### Card configuration:

We use the UNIX command *iwconfig* changing the transmit power, rate and channel settings. The *Ubiquiti SR2* card we use provides us with the option of using seven different transmit powers - 16mW, 14mW, 12mW, 10mW, 8mW, 6mW and 4mW. The card also has zero power state or an off state. It has been observed that the max transmit power of 16mW is in fact not actually 16mW but quite less. So we used only six transmit powers.

The graph in Figure 3.4 shows the average RSSI versus the corresponding transmit power for link  $S_1R_1$ , in location1. We can clearly observe that there exists a linear relation between the transmit power and the received signal strength. This justifies the use of controlling transmit power settings to actually change the signal-strength of a particular link.

### 3.2.5 Measurement Procedure

We perform various experiments by varying the transmit power settings of the sender and the interferer. In each experiment, we assign the same transmit rate (e.g. 1Mbps, 5.5Mbps) to both sender and the interferer. For each rate we vary the sender and interferer parameters as follows. We first vary the sender transmit power, keeping the interferer transmit power constant at minimum transmit power value. We then keep the sender transmit power constant at maximum transmit power and vary interferer transmit power. Thus, for every experiment, we are creating a link-pair with different properties, and therefore, we can consider each experiment as a separate link pair. Each experiment is now characterized by (a) the transmit rate used, (b) the sender transmit power, and (c) the interferer transmit power.

During the measurements, the receiver  $R_1$  acts as the central control node, and passes the experiment parameters to the other two nodes. The following is the sequence of events at each node during the measurements. Each node starts by checking reachability with its neighboring nodes. Once the neighboring node is up and reachable, a TCP connection is established between  $R_1 - S_1$  and  $R_1 - S_2$ . Network Time Protocol (NTP) is used for time synchronization between the three nodes to synchronously start the experiment.  $R_1$  acts as

the time server, and the other two nodes synchronize their clock to  $R_1$ 's clock using standard *ntpdate* command. The observed synchronization error is the order of hundreds of microseconds. This error is acceptable because of the fact that the time taken for transmission of a single UDP packet of size 1000 bytes is of order of few milliseconds. This will ensure that the interferer starts its transmission before the sender completes transmission of its first packet, or vice versa. The NTP server is disabled during the actual measurements.

After the TCP connections have been established, each node sends the next experiment number it has to perform to the central node  $R_1$ .  $R_1$  then decides upon the next experiment to be performed (each experiment number here is associated with a set of parameters: transmit rate, interferer and sender signal strengths). The central control node also decides upon a future timestamp called *experiment start-time* and communicates it to the other two nodes. Figure 3.5 depicts the flow of events at node  $S_2$  during measurements.

A measurement starts by nodes sleeping exactly up to *experiment start-time*. At experiment start-time both  $S_1$  and  $S_2$  start simultaneous transmission of continuous stream of UDP packets of size 1000 bytes for 30 seconds, while  $R_1$  listens in monitor mode. We call this the stage-1 measurement. This will give us the packet error rate of link  $S_1R_1$  in the presence of interferer  $S_2$ . Then  $S_1$  transmits alone for 30 seconds, while  $S_2$  and  $R_1$  listening. This is followed by  $S_2$ 's transmission. This gives the RSSI information of  $S_1$  and  $S_2$  respectively. This is the stage-2 measurement.

In summary, the experiments measure interference in relation with the difference in the RSSI of the sender signal and the interferer signal at particular receiver, or simply the signal to interference ratio (SIR). We have also performed similar kind of experiments for 802.11g, but we focus on the study of interference in 802.11b only.

### 3.3 Interference Estimation using Signal to Interference Ratio

In this Section, we use the above measurement data to propose and evaluate a way to estimate interference, which can be used in the generation of interference map.

### 3.3.1 Signal to Interference Ratio (SIR)

*Signal to Interference and Ratio (SINR) is the ratio of the signal strength of the wanted signal to that of the background signal from other links and noise.* For packet to be successfully received on a particular link, its SINR value should be above some threshold. This threshold depends on the transmit rate. The delivery probability of a particular link increases with SINR.

It has been well established that any wireless link has a particular error rate associated with it. The error rate a link experiences depends on its RSSI values and in particular the Signal to Interference plus Noise Ratio (SINR) values. In this work, we consider only the Signal to Interference Ratio (SIR) for interference estimation instead of SINR. This is because the interference we expect, is much higher than the background noise.

According to the FRACTEL measurement study [8], out-door wireless links generally have some inherent but quantifiable variability. That is, a link is associated with a band of RSSI values instead of a single RSSI. As, SIR is practically the difference between the sender and receiver RSSI in dBm, and the sender and receiver RSSI are not single values but form a distribution, the SIR also forms a distribution. The SIR distribution between two nodes with RSSI distribution  $P_x$  and  $P_y$  is given by

$$P_{SIR}(\alpha) = \sum_{k=-K}^K P_x(k) + P_y(k - \alpha)$$

The following Figure 3.6 shows the example SIR distribution calculated using above formula. It shows the RSSI distribution of link  $S_1R_1$  and  $S_2R_2$  for a 1Mbps and location1 and the corresponding SIR graph.

### 3.3.2 Estimation of Delivery probability using SIR

Theoretically the SINR versus delivery probability graphs are ‘S’ shaped curves with a sharp transition from high delivery probability to a low delivery probability. Both [5] and [11] has also experimentally shown that the SINR values for which the delivery probability is between 10% and 90% is only 3dB. So, if the SINR of a packet falls above this range we can say that there is a high chance that the packet will be received. And if the packet’s SINR is below, it

would be lost. Figure 3.7 shows the SINR versus delivery probability curves observed during a controlled cable experiment performed in Roofnet[5].

Now, we can use this SIR versus delivery probability curve, and the approximated SIR distribution to find the delivery probability of the link. Following formula gives the discrete approximation of the delivery probability of a link with SIR distribution  $P_{SIR}$  as

$$DeliveryProbability = \sum_{\alpha=-X}^X P_{SIR}(\alpha) * DP(\alpha)$$

Where  $DP$  represents the SIR versus the delivery probability curve, and  $X$  is the limit SIR value in dB.

### 3.3.3 Results and explanations

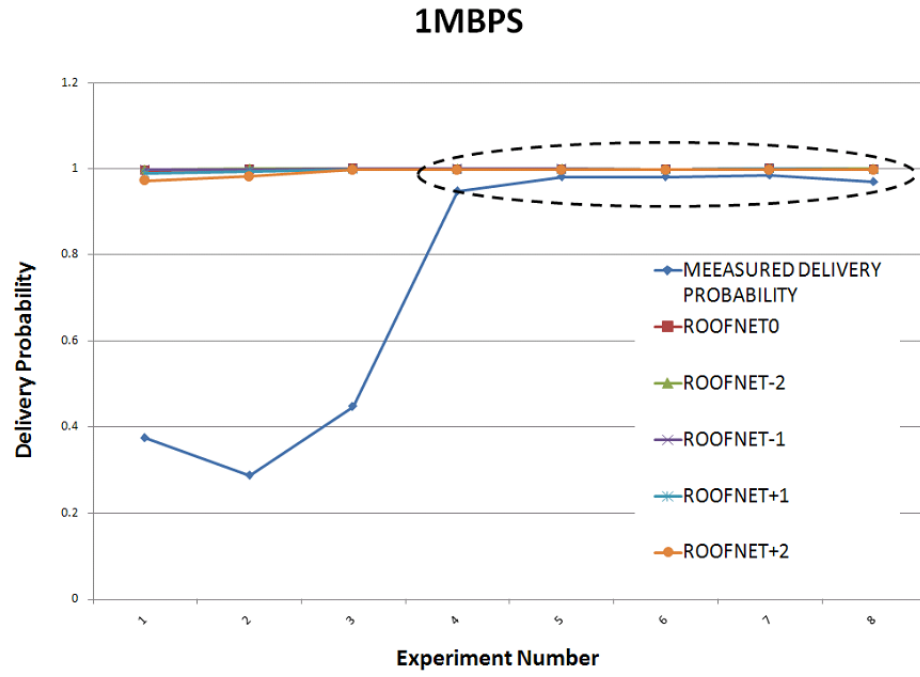
The above hypothesis is evaluated as follows. We first compute the throughput of link  $S_1R_1$ , for each experiment under the influence of interferer  $S_2$  from the Stage-1 (simultaneous transmissions). We then calculate the individual RSSI distributions from Stage-2 (individual transmissions), where the sender and interferer broadcast individually. We calculate the SIR by using method.

The actual delivery probability is calculated as the ratio of link throughput in presence of interference to the actual link throughput. We compare this with the delivery probability predicted using the SIR values from Stage-2. For the purpose of evaluation we take five different SIR versus delivery probability curves for each rate. These are the curves with the steep transition according to the theoretical values (as obtained roofnet cable experiment), 1dB to the left of the actual theoretical values, 2dB to the left of it, 1dB to the right and finally 2dB to the right. We can approximate the SIR versus the delivery probability graph as a tri-linear curve, with a steep linear transmission from 10% delivery probability to 90% delivery probability at the center, another linear transmission from 0% delivery probability to 90% delivery probability of width 4dB on left and final linear transmission from 90% delivery probability to 100% of width 4dB on right. We call these curves roofnet, roofnet-1, roofnet-2, roofnet+1 and roofnet+2 respectively.

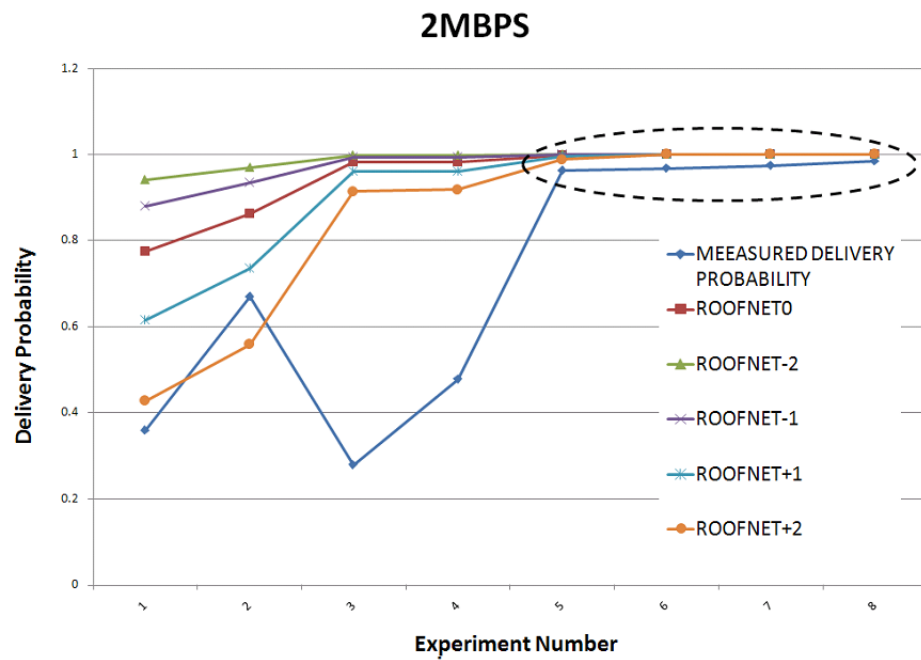
The comparison with only roofnet did not match the expected results. Therefore, we

conjectured the difference could be due to the fact that roofnet's [4] measurements were done on a different card. So we considered roofnet, roofnet-1, roofnet-2, roofnet+1 and roofnet+2 also for evaluation.

The set of graphs in Figures 3.8 and 3.9 show the predicted and actual delivery probability measured in h12 location for four rates 11Mbps, 5.5Mbps, 2Mbps and 1Mbps. Each graph shows the delivery probabilities for 8 different experiments performed with constant interferer signal strength and varying sender signal strength.

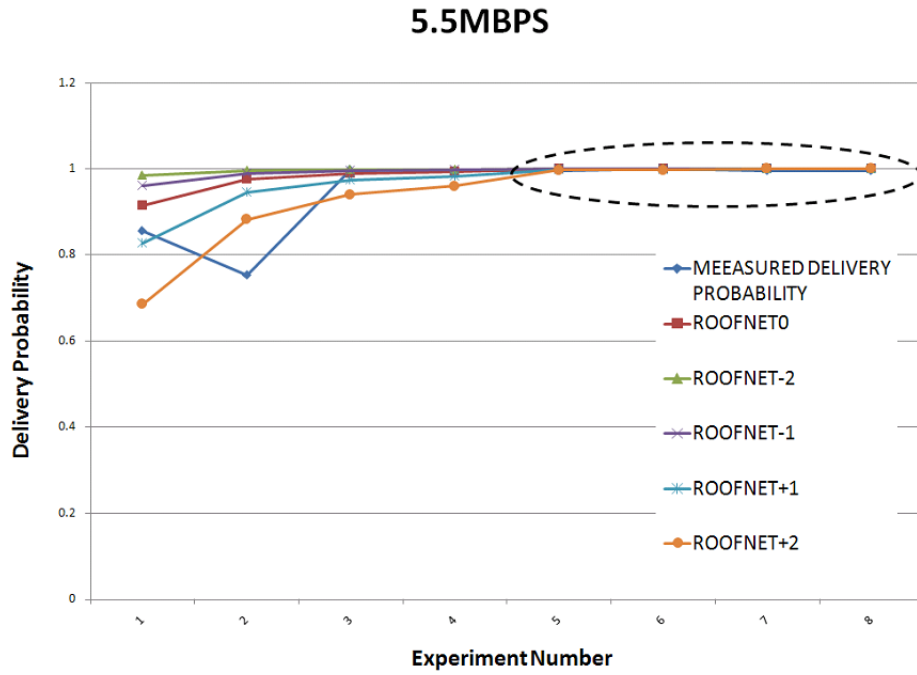


(a) 1MBPS

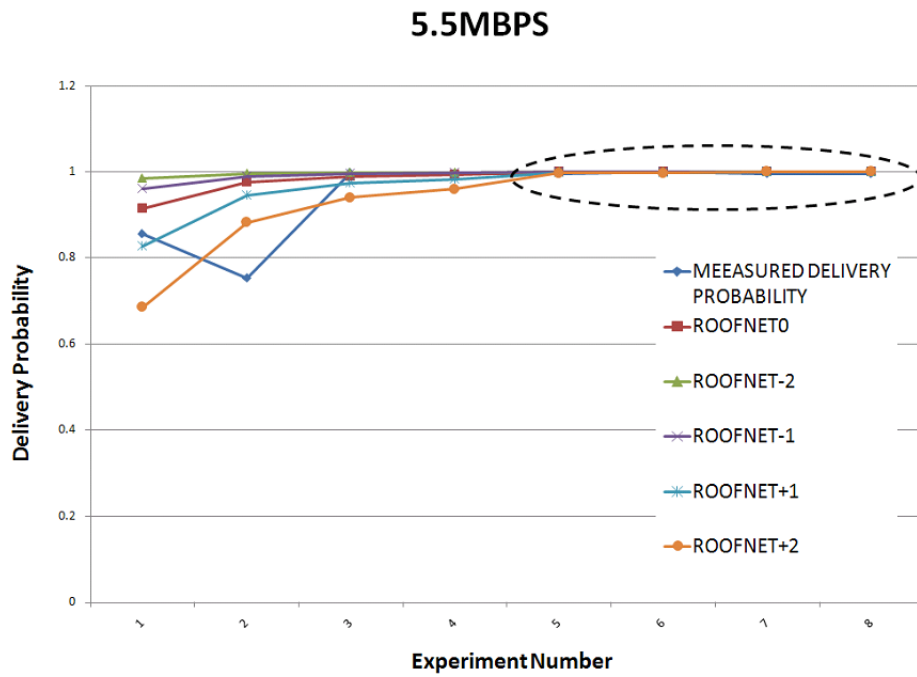


(b) 2 MBPS

Figure 3.8: Predicted vs Measured Delivery Probability



(a) 5.5MBPS



(b) 11 MBPS

Figure 3.9: Predicted vs Measured Delivery Probability



We observe that, though the predicted graphs generally follow the same trend as that of the actual measured delivery probability, the accuracy is not up to the mark. Though we are able to accurately predict the cases with high delivery probability (close to one) and low delivery probability (close to zero), the accuracy of the prediction comes down when the actual delivery probability is in between.

### Area analysis

Why is the accuracy affected, when the link is in the transition from high delivery probability to low delivery probability? To analyze this, we have to find out if the RSSI distribution of the link S1-R1 from stage1 is similar to that of the RSSI distribution from the stage2. We need to check whether a link exhibits same kind of RSSI distribution over time, i.e., we need to verify its stability

For this, first divide the 30 second data from each experiment into six bins of five seconds each. Then check if the six distributions of Stage1 simultaneous transmissions are similar to the six corresponding distributions of Stage2 individual transmission. And also check if the RSSI distributions of the six bins of S1 and S2 in stage2 are same amongst themselves. As a metric of accuracy to compare two PDFs we simply compute the area between them in the same graph (in 1dB units). This area can vary from zero, for similar distributions to a maximum of two. This is because the area under a given PDF curve is 1, by definition.

We notice that, for our experiments the area between the curves is not exactly close to zero, but varying from close to zero to as high as 1 and in some rare cases it shoots up beyond that. This shows us that there is not as much stability in the RSSI that we require for this kind of prediction. That is, though the general band of RSSI may be successfully calculated, the distribution inside this might vary like depicted in Figure 3.10 below. The Figure shows the RSSI distributions of six successive five-second windows of same transmit power setting for 1Mbps and location1. We can clearly observe that, though all the distributions start around -65dBm and end near -58dBm, the distribution of RSSI values inside this band varies a lot. This effect is of special significance when the link falls in the steep region of the SIR versus delivery probability curve, because a small variation in the distribution in this region, causes a huge difference in the delivery probability.

Thus, owing to the instability of the RSSI during smaller time periods, it is not possible to accurately predict the link delivery probability for any future point with only a small duration of measurement. We now, try to use the fact that only the general trend of delivery probability can be estimated for classification of links. This is discussed further in next Section.

### 3.4 Three-way Classification using 2.5th percentile and 97.5th percentile SIR values

#### 3.4.1 The three - way classification

Here we try to propose and evaluate a three-way strategy to classify the inter-link interference. Each link is divided into one of the three categories with respect to a particular interfering link or simply an interferer. To classify these link-pairs accordingly we use the 2.5<sup>th</sup> and 97.5<sup>th</sup> percentile SIR band. This band is intended to cover most of the variability of SIR, ignoring the outliers . The three categories are

1. Non-Interfering Links
2. Interfering Links
3. Intermediate / Variable Links

We propose that a link-pair with its SIR band completely above the steep region (2.5<sup>th</sup> and 97.5<sup>th</sup> percentile region) of the SIR versus delivery probability curve can be classified as non-interfering links. Theoretically, any packet with SIR in this particular band can be successfully received with a very high probability. As 95 percent of the packets are in this region the delivery probability can be predicted to be close to 0.95 and thus the links are non-interfering. Similarly if the SIR band is completely below the steep region, the links can be classified as interfering. Though there would be some variation of distribution inside the SIR band, the classification of the links will not change, because all the packets within the band have similar delivery probability.

Finally we classify the link-pair whose SIR band is neither completely above or completely below this particular Section as variable links. Because of the steep curve in this band, the

delivery probability of these links can vary a lot depending on the exact distribution of the SIR values during that time. Though the accurate behavior cannot be determined, we can surely note that there would be some degree of interference among the links and they cannot be operated simultaneously.

During the classification it is really important that there are no false negatives (the links that are classified as non-interfering or variable but are in fact interfering) because, these are the links which would be simultaneously operated during spatial re-use. To avoid these false negatives, we conservatively expand the measured SIR band by 1dB on either side. There might be some false positives (the links which actually may not interfere, but classified as interfering or intermediate links) in this case, but it's a trade off.

### 3.4.2 Results and Analysis

To test the above classification strategy, we again divide the 30 second measurements into sets of five second bins and consider each of them as a separate experiment. We have six separate bins of similar kind in stage-1 and 12 bins (six for  $S_1R_1$  and six for  $S_2R_1$  each). We compare the actual measured delivery probability of the six bins from stage-1 and the classification done using the SIR computed by the six bin pairs in the stage-2. This is similar to performing six experiments with similar parameters, only interleaved in time. This particular approach will provide us with increased number of data points for proper analysis. We also use five different Delivery Probability vs SIR curves for calculation of steep region boundaries. These we call Roofnet, Roofnet +1, Roofnet +2 and Roofnet -1 corresponding to the curve obtained using the Roofnet cable experiment described earlier, the curve 1dB to the right of it, the curve 2dB to the right of it and finally the curve 1dB to the left of it. The table 3.3 shows the steep region boundaries we considered for classification obtained by roofnet cable experiment

We present these classification results separately for four sets of nodes described below.

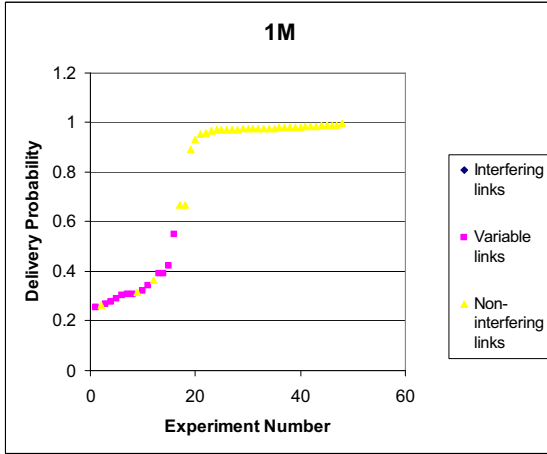
1. Location 1, with constant sender signal strength and varying interferer signal strength.
2. Location 1, with varying sender signal strength and constant interferer signal strength.
3. Location 2, with constant sender signal strength and varying interferer signal strength.

<b>Rate</b>	<b>Lower Boundary (97.5<sup>th</sup> percent value)</b>	<b>Upper boundary (97.5<sup>th</sup> percent value)</b>
1Mbps	-2	2
2Mbps	1	5
5.5Mbps	3	7
11Mbps	6	10

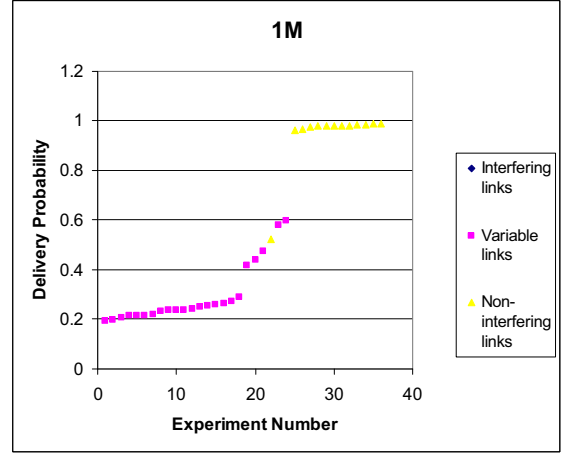
Table 3.3: SIR Band for the steep region (Roofnet) : Source [5]

4. Location 2, with varying sender signal strength and constant interferer signal straight.

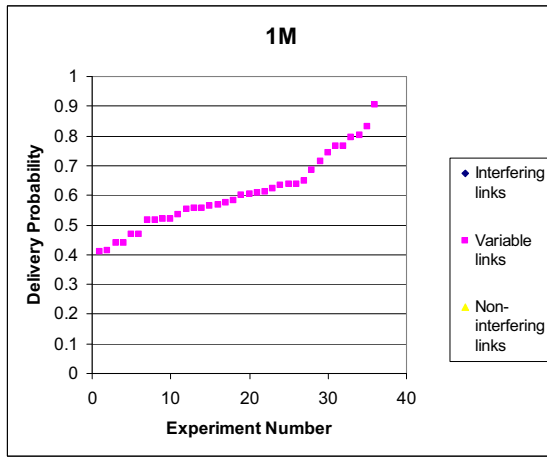
Figure 3.11 shows the classification of 1Mbps links based on the Roofnet+2 curve. This particular curve gives the best classification results for 1Mbps.



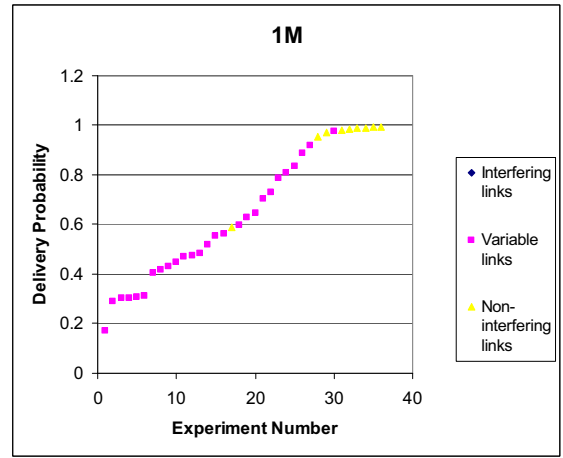
(a) Location1 (type 1)



(b) Location1 (Type 2)



(c) Location2 (type 3)



(d) Location2 (type 4)

Figure 3.11: Three way classification of 1Mbps links

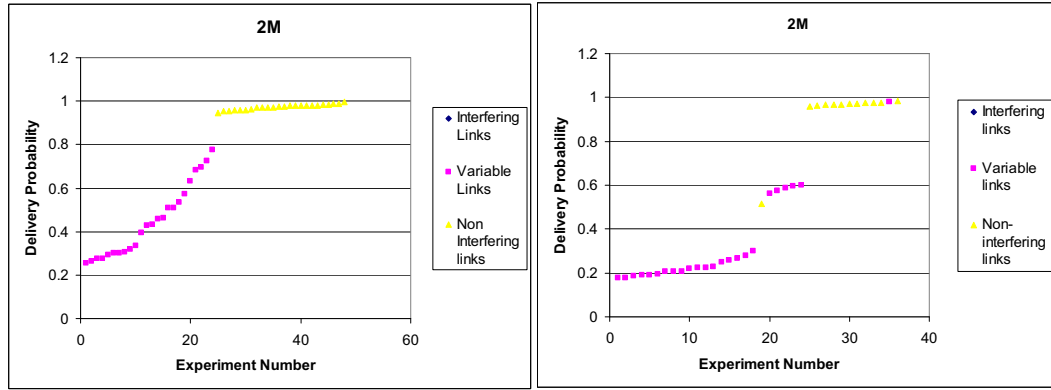
The table 3.4 below shows the accuracy obtained using the five different SIR versus delivery probability curves described earlier. To calculate the accuracy, we manually classify the links according to the measured delivery probability. If the delivery probability is above 0.95, we consider the link-pair as non-interfering. On the other hand, if the delivery probability is less than 0.1, it is considered as interfering. All the other links are classified as variable links. Now, we compare this manual classification using the measured delivery probability with the actual classification based on SIR band and report the accuracy.

Type of experiment	Number of Experiments	Accuracy (Roofnet)	Accuracy (Roofnet -1)	Accuracy (Roofnet +1)	Accuracy (Roofnet -2)	Accuracy (Roofnet +2)
Location 1 (Type 1)	48	66.6%	60.4%	81.25%	58.33%	<b>87.5%</b>
Location 1 (Type 2)	36	75.0%	61.1%	97.2%	44.44%	<b>97.2%</b>
Location 2 (Type 3)	36	86.1%	91.7%	91.7%	69.44%	<b>100%</b>
Location 2 (Type 4)	36	88.0%	80.5%	91.7%	77.78%	<b>94.4%</b>
All	156	78.20%	72.4%	89.7%	59.62%	<b>94.8%</b>

Table 3.4: Accuracy for three-way classification 1Mbps

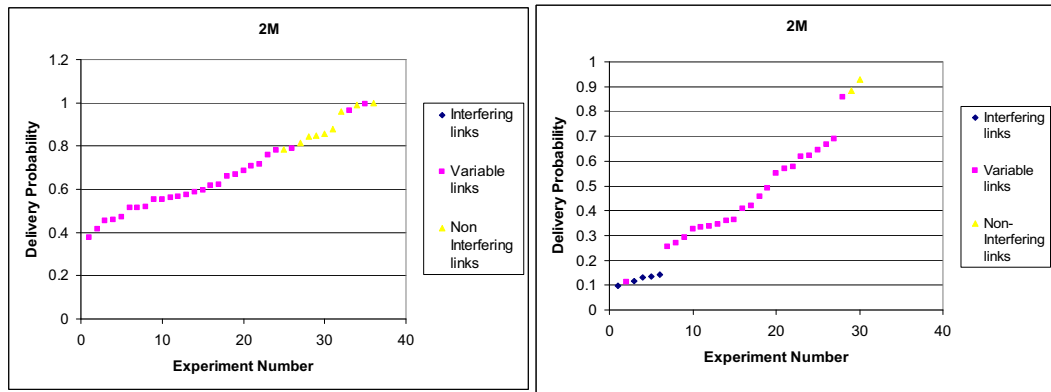
It shows that, we can obtain an average accuracy of 95 percent, with the three way classification. The accuracy goes up further if we consider only the links which are judged as non-interfering and are in fact interfering.

The following figures show the three way classification for 2Mbps, 5.5Mbps and 11Mbps respectively. The tables below them show the corresponding accuracy values. From figures 3.12 and 3.13 we can observe a perfect 3-way classification for both 2Mbps and 5.5Mbps, though the accuracy seems a bit low (about 90%). This is because of the links which are classified as variable links but has delivery probability greater than 0.95. As we discussed earlier, this is caused due to the conservative nature of the classification we have used. The actual number of false negatives in the classification is even less. 2Mbps has 5.3% false negatives (94.7% accuracy) and 5.5Mbps has only 2% false negatives (98% accuracy). Similarly Figure 3.14 shows the classification of 11Mbps data. We can observe that for the experiments performed in location 2, there are lots of points which are classified as interfering but should be classified as variable links as they exhibit delivery probabilities greater than 0.1. The actual false negative cases for this rate cannot be analyzed because there are very few links that are interference free. We can also observe that for classification of 1Mbps, 2Mbps, 5.5Mbps and 11Mbps, accuracy is highest for roofnet+2, roofnet, roofnet-1 and roofnet+2 respectively. That is, for some rates we are getting better accuracy for roofnet and in some cases we are getting better accuracy for roofnet+2. This difference is perhaps because of the difference in the wireless cards we used.



(a) Location1, Type1

(b) Location 1, Type 2



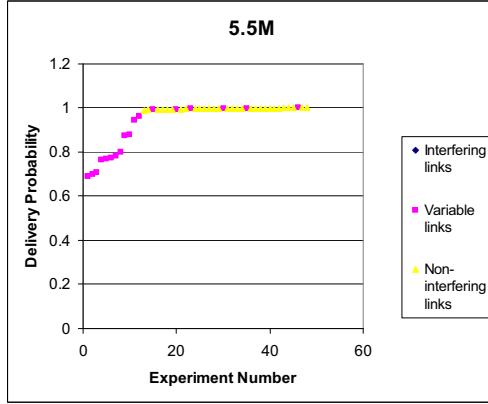
(c) Location 2, Type 3

(d) location 2, Type 4

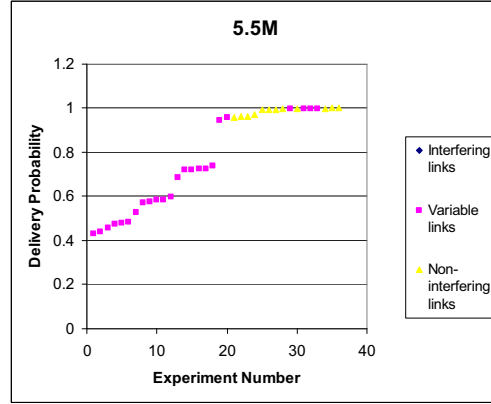
Figure 3.12: 3-way classification for 2Mbps

Type of experiment	Number of Experiments	Accuracy (Roofnet)	Accuracy (Roofnet -1)	Accuracy (Roofnet +1)	Accuracy (Roofnet -2)	Accuracy (Roofnet +2)
Location 1 (Type 1)	48	<b>97.9%</b>	91.7%	95.8%	83.33%	85.4%
Location 1 (Type 2)	36	<b>94.4%</b>	97.2%	86.1%	88.89%	83.3%
Location 2 (Type 3)	36	<b>77.8%</b>	77.8%	75.0%	80.56%	75.0%
Location 2 (Type 4)	30	<b>90.0%</b>	90.0%	86.7%	86.67%	83.3%
All	152	<b>90.7%</b>	89.3%	86.7%	84.67%	80.0%

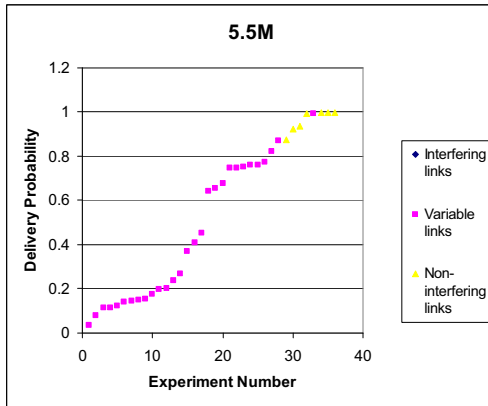
Table 3.5: Accuracy for three-way classification 2Mbps



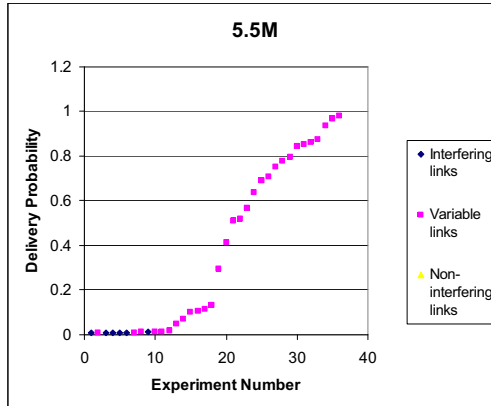
(a) Location1, Type1



(b) Location 1, Type 2



(c) Location 2, Type 3



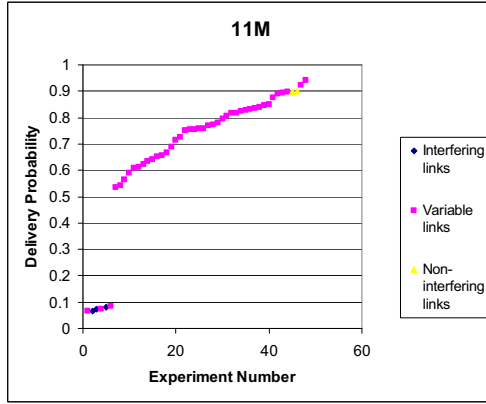
(d) location 2, Type 4

Figure 3.13: 3-way classification for 5.5Mbps

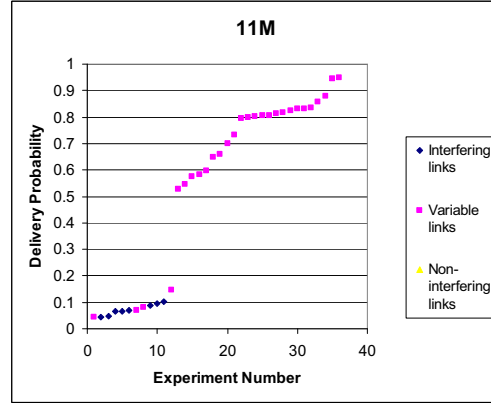
Type of experiment	Number of Experiments	Accuracy (Roofnet)	Accuracy (Roofnet -1)	Accuracy (Roofnet +1)	Accuracy (Roofnet -2)	Accuracy (Roofnet +2)
Location 1 (Type 1)	48	66.6%	<b>85.4%</b>	75.0%	91.67%	68.7%
Location 1 (Type 2)	36	77.08%	<b>86.1%</b>	69.4%	94.44%	58.3%
Location 2 (Type 3)	36	75.1%	<b>88.9%</b>	75.0%	86.11%	72.2%
Location 2 (Type 4)	36	88/0%	<b>88.9%</b>	88.9%	72.22%	88.8%
All	158	80.8%	<b>87.2%</b>	76.9%	86.54%	71.7%

Table 3.6: Accuracy for three-way classification 5.5Mbps

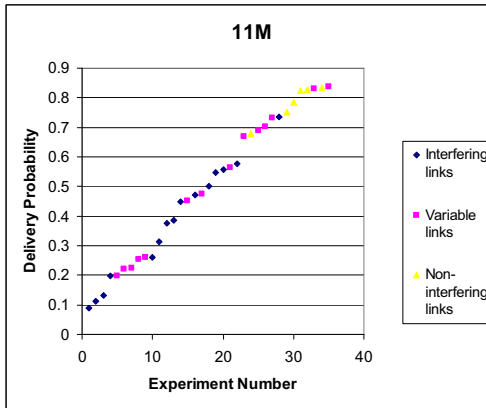




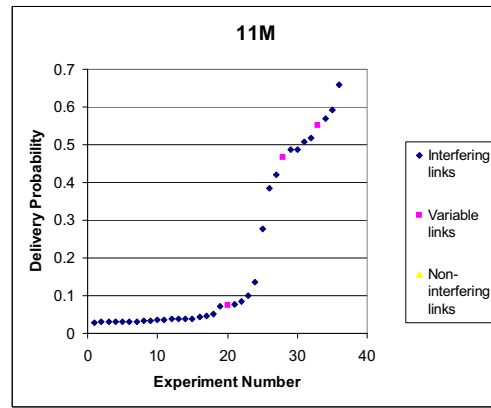
(a) Location1, Type1



(b) Location 1, Type 2



(c) Location 2, Type 3



(d) location 2, Type 4

Figure 3.14: 3-way classification for 11Mbps

Type of experiment	Number of Experiments	Accuracy (Roofnet)	Accuracy (Roofnet -1)	Accuracy (Roofnet +1)	Accuracy (Roofnet -2)	Accuracy (Roofnet +2)
Location 1 (Type 1)	48	72.9%	68.7%	83.3%	68.75%	<b>95.8%</b>
Location 1 (Type 2)	36	75.0%	72.2%	91.6%	72.22%	<b>83.3%</b>
Location 2 (Type 3)	36	75.0%	66.6%	75.0%	66.67%	<b>83.3%</b>
Location 2 (Type 4)	36	83.3%	97.2%	75.0%	97.22%	<b>72.2%</b>
All	158	76.9%	76.9%	80.7%	76.92%	<b>84.6%</b>

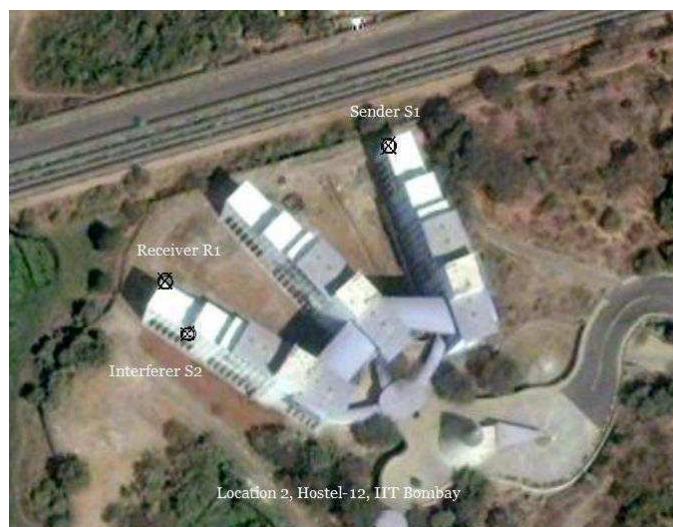
Table 3.7: Accuracy for three-way classification 11Mbps

### 3.5 Conclusions

In summary, we have performed measurements to study inter-link interference and its relation with the sender and interferer signal strengths. We calculated the approximated SIR distribution based on these measurements. We then used the SIR versus delivery probability curves (modified as 5 different versions as discussed previously) from the roofnet measurements, to determine the interference estimation strategy. The following are some of the important conclusions of the measurement study we have performed.

- The accurate prediction of delivery probability based on the approximated SIR is not possible. This is because of the variability in the link RSSI, which follows a complete random pattern.
- The inaccuracy is more for the cases with intermediate delivery probability; this is because the variable RSSI values affect the most when the SIR band coincides with the steep region of the SIR versus delivery probability curve.
- It is possible to classify the link-pairs into one of three categories: interfering, non-interfering and variable links, based on the 97.5<sup>th</sup> and 2.5<sup>th</sup> percentile values of SIR band and the SIR versus delivery probability curve. The accuracy of this classification is shown to be around 90% in our environment.

The accuracy of the classification might still be improved by using the proper SIR versus delivery probability calculated from controlled calibration experiments using the ubiquity cards.



(a) Location1 - Hostel12, IIT Bombay



(b) Location2 - Academic area, Hostel 12

Figure 3.3: Experiment Locations[Reference: Google earth images]

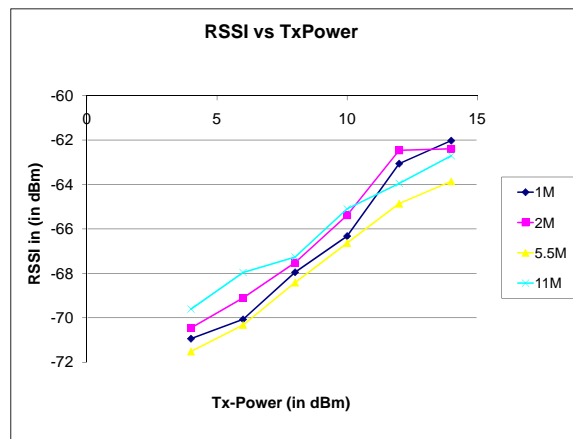
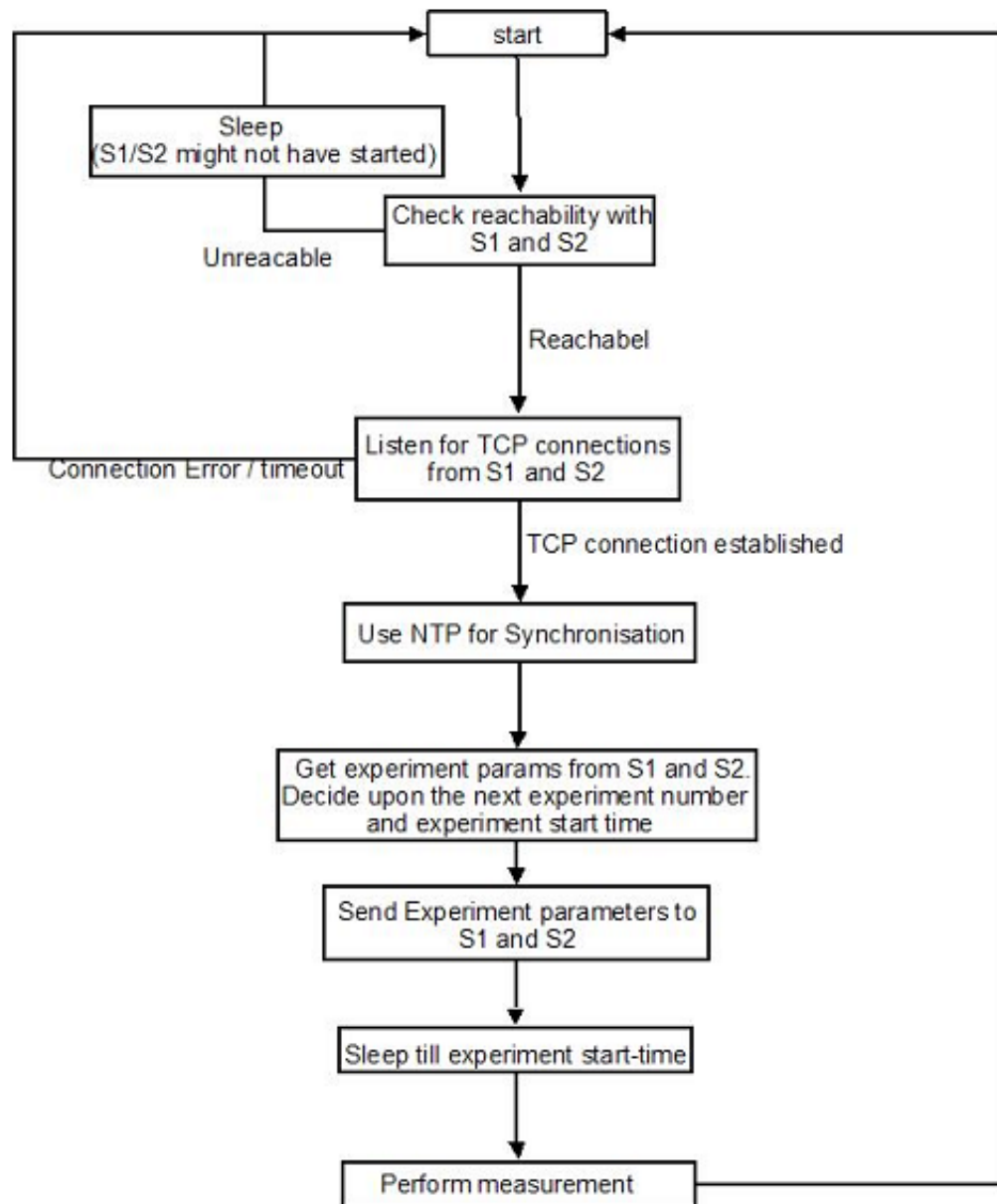


Figure 3.4: Average RSSI versus TxPower graph for S1-R1 Link, Location1

Figure 3.5: Flow of events at  $R_1$  (measurement procedure)

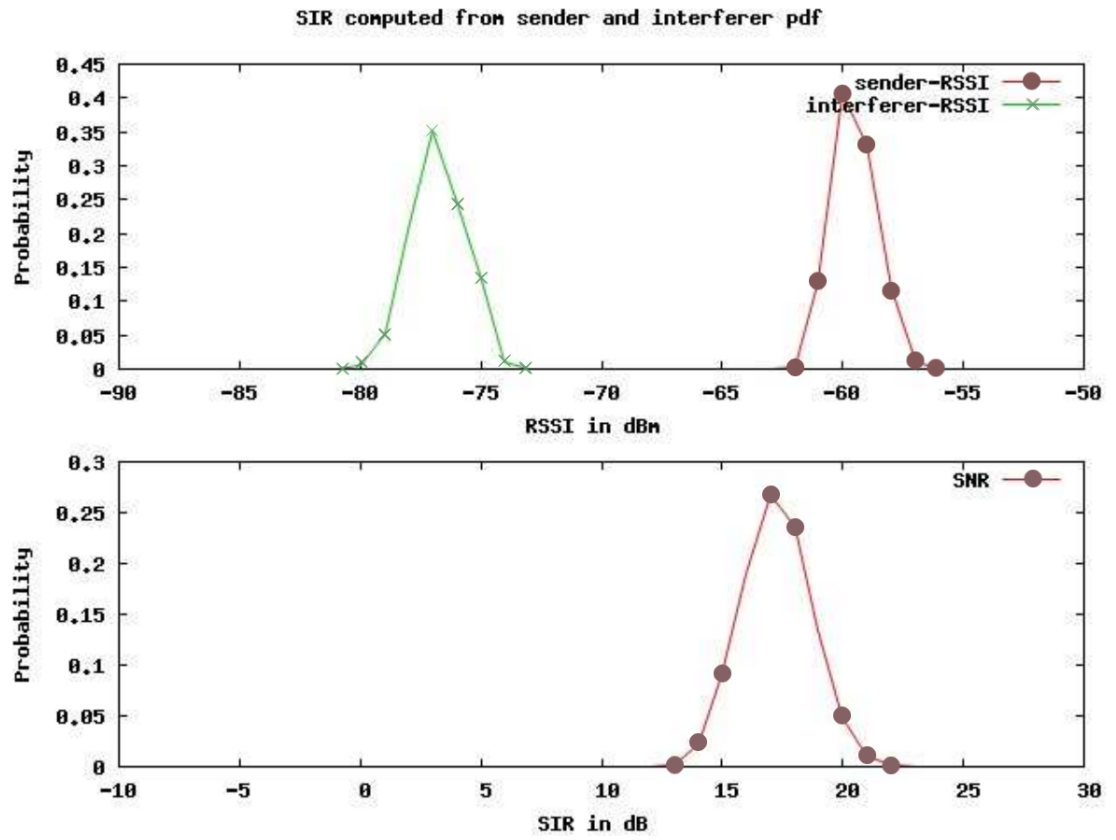


Figure 3.6: SIR distribution computed using convolutions

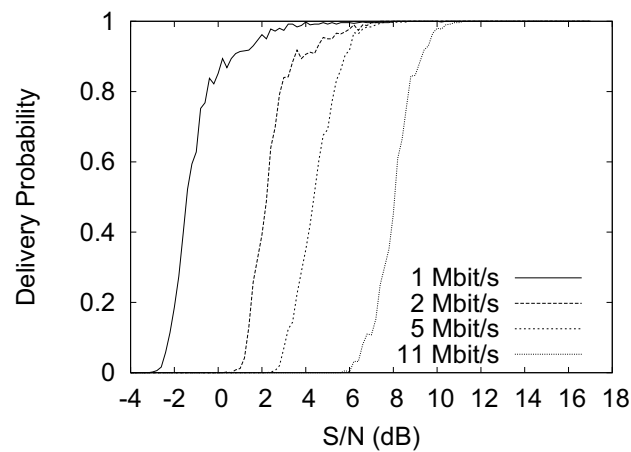


Figure 3.7: SINR versus Delivery Probability measured during an emulator experiment. Source:Roofnet measurement study [5].

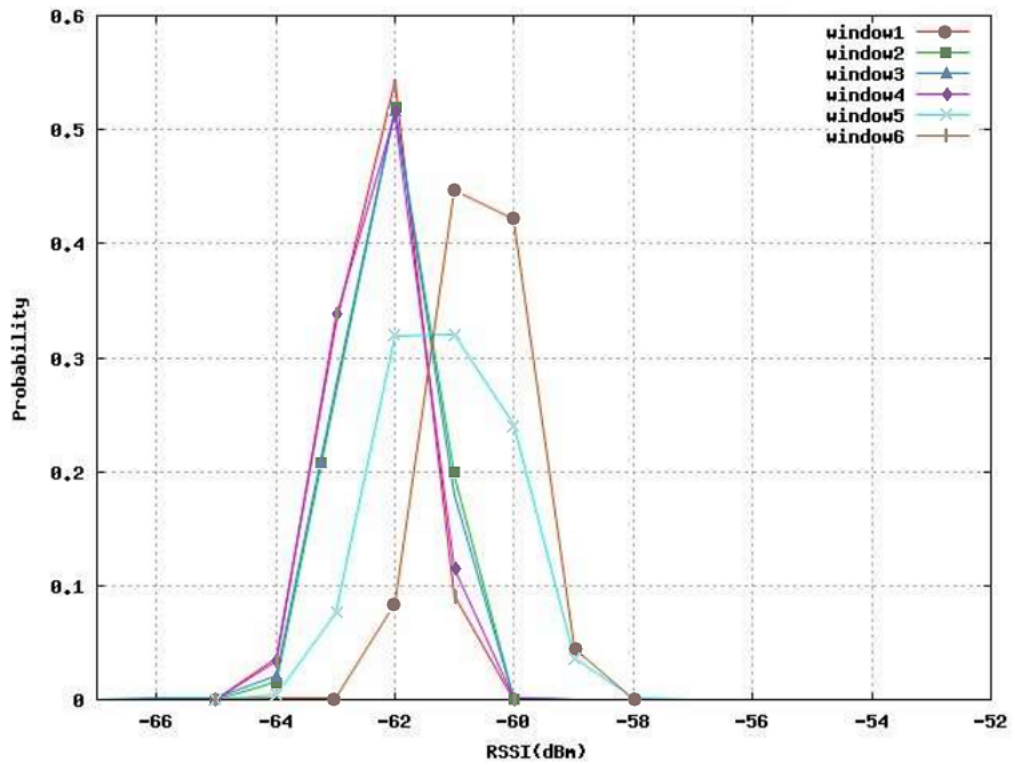


Figure 3.10: Successive RSSI distributions for same link

## Chapter 4

# Time - Period analysis

To completely automate the interference map generation, it is not enough to just estimate interference and derive a static interference map based on it. We know from the previous studies that wireless links are not stable but have a lot of variability, which establishes the necessity for timely repetition of measurements. For timely repetition, we need to determine the interval between the two successive measurements as well as the duration of the each measurement.

We now answer two important questions here in this chapter.

1. What should be the time-period ( $T$ ) (interval between two successive measurements) of measurements, such that the error during the prediction is minimized?
2. What should be the duration ( $t$ ) of each measurement, such that we collect enough information to predict the RSSI pattern for next  $T$  time?

To answer these questions, we must analyze the wireless data for longer duration.

### 4.1 Long Duration Experiments

#### 4.1.1 802.11 (WiFi)

For the time series analysis of 802.11 links, we use the long duration data collected during the FRACTEL measurement study [8]. The data is collected continuously for 48/24hr duration over medium distance wireless links in six different positions. During these experiments



the transmitter sends packets at an inter packet interval of 20 milliseconds and at full rate (11Mbps). The data is collected over two separate locations, with receiver at three different positions in each of the location. The following is the brief description of locations taken from [8]. Refer to FRACTEL measurement study for further details of the measurements.

- Location 1 (ACES Type II) : This location consists of several rows of two-storeyed houses on campus. There are a number of trees in the vicinity of the houses that are much taller than the house. Three separate 48hr duration experiments are conducted in this location. Let us call these locations - pos-1, pos-2 and pos-3.
- Location 2 (SBRA) :This location is the student residence; it has four rows of three-storeyed tall buildings along with few very short trees in the vicinity. Three 24hr experiments are conducted in this location. We call these locations - SBRA position 1, SBRA position 2 and SBRA position 3

#### 4.1.2 802.15.4 (Sensor Networks)

We also collected and analyzed longer duration experiments for 802.15.4. We used Motiv T-mote sky motes with CC2420 Chipcon radio for measurements. We used the TinyOS for programming the sender and the receiver. During each experiment, the sender transmits packets with inter-packet gap of 20 milliseconds. The receiver uses a TOSBase program supplied by the TinyOS distribution to receive this data and forward it to the laptop connected to the receiver using a long USB cable.

The data is collected over nine separate locations for 24hr duration each. We have chosen the locations for the measurement such that they cover different kinds of environments, where there is a possibility for establishment of medium distance links. Following are the locations at which the 802.15.4 data is collected.

##### Corridor Type locations

1. *Corridor, Hostel 12, IIT B*: This location is a long corridor surrounded by concrete walls on all four sides. The sender and receiver are 55 meters apart with a clear line of sight.

There is no presence of external interference, but there is irregular people movement in the line of sight.

2. *Corridor, 4th Floor, KReSIT Building, IITB (with Line of Sight)*: This location is a large hall-way-type corridor with pillars around. The sender and receiver here are 25 meters apart. There is a clear line of sight with some people movement. There are a lot of WiFi sources around which act as external interference.
3. *Corridor, 4th Floor, KReSIT Building, IITB (with Non - Line of Sight)*: This is the same location as above, but with the nodes placed such that there is no line of sight. The distance between the sender and the receiver is about 10 meters.

### Outdoor Locations

1. *Roof-top, Hostel 12, IITB*: In this location, the nodes are placed on top of two tall buildings, 40 meters apart. There is a clear line of sight and presence of tall buildings around will account for some multipath. There is small amount of 802.11 interference.
2. *Roof-top, KReSIT, IITB (with Line of Sight)*: The nodes in this location are placed on top of water tanks on KReSIT building. The distance between the nodes is 35 meters. There is some 802.11 interference but has no movement between the nodes.
3. *Roof-top, KReSIT, IITB (with Non - Line of Sight)*: This is the same location as above. The nodes are placed on the ground of roof-top without line of sight. The sender and the receiver are only 5 meters apart (as the communication is difficult without line of sight).
4. *Roof-top, GG building to KReSIT Building, IITB*: This is the longest link we could establish without using external antennas. The sender and the receiver are around 130 meters apart and placed on top of two tall buildings. There is a clear line of sight between the sender and the receiver. There is some amount of foliage in the environment, but is clear from line of sight.

### Indoor Location

1. *Computers lab, KReSIT, IITB*: In this location the nodes are placed inside our laboratory. They are placed five to six meters apart and do not have a clear line of sight between them. There is a lot of people movement along with a lot of change in the environment.

### Foliage Location

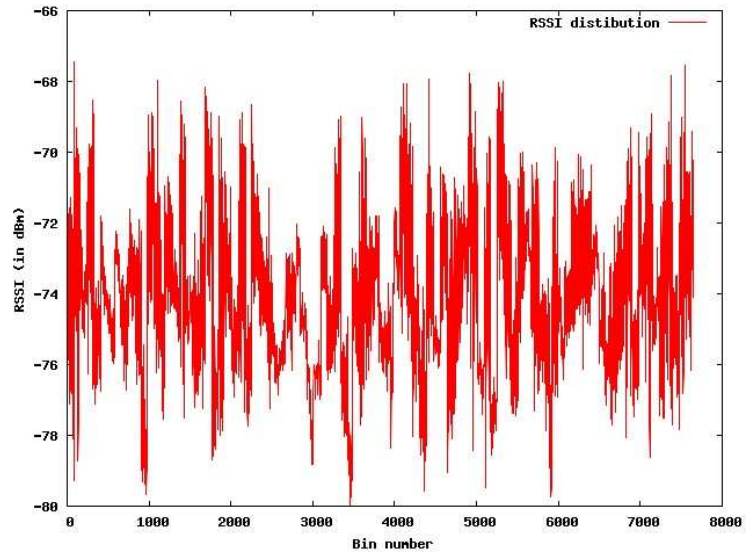
1. *Roof-top, CSE building- CC building, IIT Kanpur*: The nodes are placed on top of CSE building and CC building with lots of foliage in the line of sight. The sender and receiver are separated by huge tree. The distance between the two nodes is around 30 meters. The location also has external interference from WiFi.

The RSSI values collected for each of these links (both in 802.11 and 802.15.4) show variability and act as a discrete function of RSSI over time or simply a time-series. We now do some basic time series analysis on this long duration data and try to determine if it is associated with any pattern, that can help us to determine  $T$  and  $t$  values.

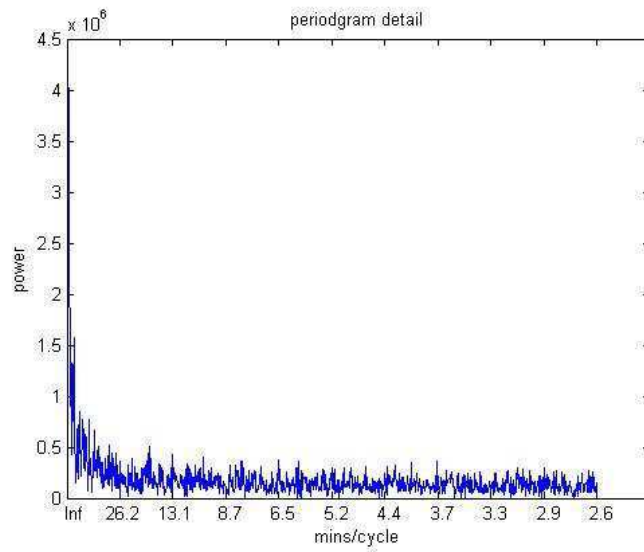
## 4.2 Spectral Analysis

The spectral analysis is based on the presumption that the data points collected over time may have some internal structure. For this purpose we first convert the time series data into frequency domain. This helps us in finding any patterns that are associated with wireless links. We use well known Discrete Fourier Transforms (DFT) to convert the time series data into the frequency domain. If there is some repetitive pattern in the RSSI variations for a particular link, converting it to frequency domain will give a spiked value at that particular frequency. A significant peak will indicate presence of cycles in the time series data.

Figure 4.1(a) shows the RSSI variation measured for location1, position 2, which is the location with maximum variability. It plots the average RSSI for 1000 packet bins. And Figure 4.1(b) shows the corresponding periodogram detail obtained using the Fourier transformation. The graph plots the square of the amplitude of the frequency of each cycle versus the length of the cycle.



(a) RSSI variability (Average RSSI per 1000 packet bin)



(b) Periodogram detail

Figure 4.1: Spectral Plots for 802.11, Location 1, Position 2

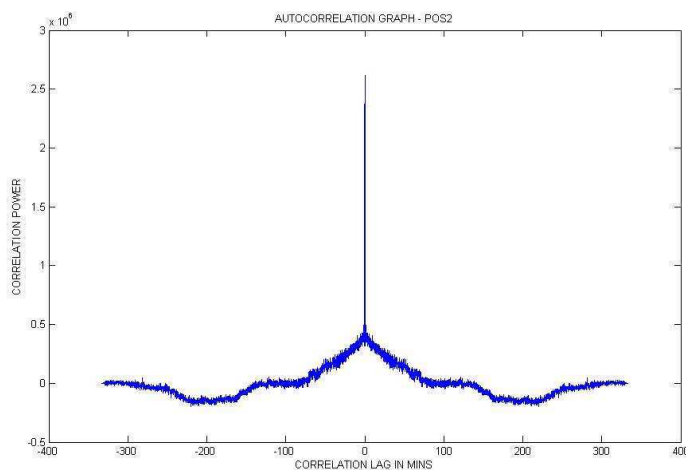


Figure 4.2: Auto - Correlogram for 802.11 link at Location 1, Position 2

From the graph we can see that the data graph shows no significant peaks, which means that there are no prominent cycles associated with it suggesting that the RSSI data might be random. We also find the auto-correlation for the time series data. Auto-correlation is a tool for finding repetitive patterns in a time series data. It gives us the self-similarity of a time series as a function of time-lag between them. The following Figure 4.2 shows the auto-correlogram for the same link as above. An auto correlogram plots the correlation power versus the time lag. The results for the other links also show the same pattern.

Both, Fourier analysis and the auto-correlogram indicate that wireless data do not have any trend or repetitive sequences. It is completely random. Further usage of smoothing and noise reduction techniques used in voice sampling might find some patterns but that kind of analysis is out of scope for this work. So, we find the measurement time period ( $T$ ) and the measurement duration ( $t$ ) by analyzing the data directly and taking an approach which is close to the interference measurement scheme we use. We describe this further in the following Sections.

### 4.3 T and t analysis

During the interference estimation strategy we described in Section 3.3, we use the RSSI band measured at some past time and classify the links based on that for next  $T$  seconds. The  $T$  and  $t$  values must be chosen such that the measurements done every  $T$  seconds for  $t$  second duration would approximate the whole link behavior with least possible error. So we calculate this error over the entire series of RSSI data (collected in the long duration experiments described above) for various values of  $T$  and  $t$ , and see which of these values give the least error keeping in mind the measurement overhead. We now explain the procedure followed in detail with examples

#### 4.3.1 T - Example

To determine the  $T$  value, we first divide the entire 24/48hr data into small windows of size  $t$ . Suppose  $t$  is fixed at 5 seconds. We now compare  $T = 1$  min versus  $T = 2$  minutes. Break up time-series into non-overlapping 5 second windows: call these windows  $w_1, w_2, w_3$  etc. So when  $T = 60$  sec, PDF measurements would be done during  $w_1, w_{13}, w_{25}, w_{37}$  etc. And when  $T = 120$  sec, PDF measurements would be done during  $w_1, w_{25}, w_{49}$ , etc. If you use  $T = 60$  sec, during  $w_2, w_3, \dots, w_{12}$ , you will use  $w_1$ 's PDF measurement as the estimate. If you use  $T = 120$  sec, during  $w_2, w_3, w_4 \dots, w_{24}$ , you will use  $w_1$ 's PDF measurement as the estimate. So the question is, whether for  $w_{13}, w_{14}, w_{15} \dots, w_{24}$ , the PDF measurement from  $w_2$  is more accurate than the PDF measurement from  $w_1$ . As a metric of accuracy for comparing of the two PDFs say  $PDF(w_i)$  and  $PDF(w_j)$ , we find the part of 2.5<sup>th</sup> to 97.5<sup>th</sup> band of  $PDF(w_j)$  that lies outside the 2.5<sup>th</sup> to 97.5<sup>th</sup> percentile values of  $PDF(w_i)$ . The idea behind the metric is that the RSSI band of  $PDF(w_i)$  should subsume the RSSI band of the  $PDF(w_j)$ . So if  $PDF(w_i)$  has a RSSI window of  $\langle x_i, y_i \rangle$  and  $PDF(w_j)$  has an RSSI window of  $\langle x_j, y_j \rangle$  then the mod-difference would be

$$\text{mod-difference} = \max(x_i - x_j, 0) + \max(y_j - y_i, 0).$$

Here also, as described in Chapter 3.3, we conservatively increase the PDF window by 1dBm on both sides. For example, if  $T = 60$  sec, the inaccuracy for window  $w_{16}$  would be:

The mod-difference between the two PDFs: (1)  $w_{16}$ 's measured PDF, and (2)  $w_{13}$ 's PDF (i.e.,  $w_{16}$ 's estimated PDF when  $T = 60$  sec) and if  $T = 120$  sec, the inaccuracy for window  $w_{16}$  would be: The mod-difference between the two PDFs: (1)  $w_{16}$ 's measured PDF, and (2)  $w_1$ 's PDF (i.e.,  $w_{16}$ 's estimated PDF when  $T = 120$  sec). So for every  $T$ , we will now have a sequence of estimated inaccuracies which can be averaged to estimate the total link inaccuracy.

### 4.3.2 $t$ - Example

To determine the duration of each experiment ( $t$ ), we take different values of  $t$  and then, see if the measurement gathers enough information for prediction. That is, we divide the time series data into non-overlapping windows of 10 seconds each. We use 10 second windows because, this typically is the time taken for a single network activity, like downloading a web page. Let us call these windows  $w_1, w_2, w_3$  etc. Now, define  $PDF(t)$  to be the PDF which will be computed by using just the RSSI data for the first  $t$  period. Compare the measured PDFs of  $w_1, w_2$ , etc with  $PDF(t)$ , for various values of  $t$ : say  $t=1$  sec, 2 sec, 5 sec, 10 sec, 15 sec, 20 sec. We also repeated this for different starting points. That is, we compare the  $PDF(t)$  measured at various points in the series for each  $t$  with the same 10 second windows calculated as said above.

### 4.3.3 Results and Conclusions

We now calculate the  $t$  first, and then use this  $t$  value to calculate the appropriate value for  $T$ . Figure 4.3 and Table 4.1 presents the results of the  $t$ -analysis for one of the long distance link, which we refer to as pos-2 in location 1 of 802.11 measurement. The Figure shows shows the cumulative results for  $t$ -analysis for pos2. It shows the average error (in terms of mod-difference described above) for 30 minute window for different  $t$  values. Each line indicate different positions from which  $PDF(t)$  is taken. The PDF is calculated at time  $N=0,1,2,5,10$  minutes from the start of the window.

Form the results we can see that, the error is pretty high for very small values of  $t$  which indicate that the small measurement duration would not be able to capture the link behavior. As the value of  $t$  increases this error becomes less as expected. We can observe that after

crossing a particular  $t$  value there is a dip in the error rate indicating that the link behavior is indeed captured. This dip occurs at various points in each of the cases but in general is less than 10 seconds. The other links we have tested also show similar pattern. So we determine that a 10 second measurement would be sufficient to capture the link behavior and can be taken as measurement duration.

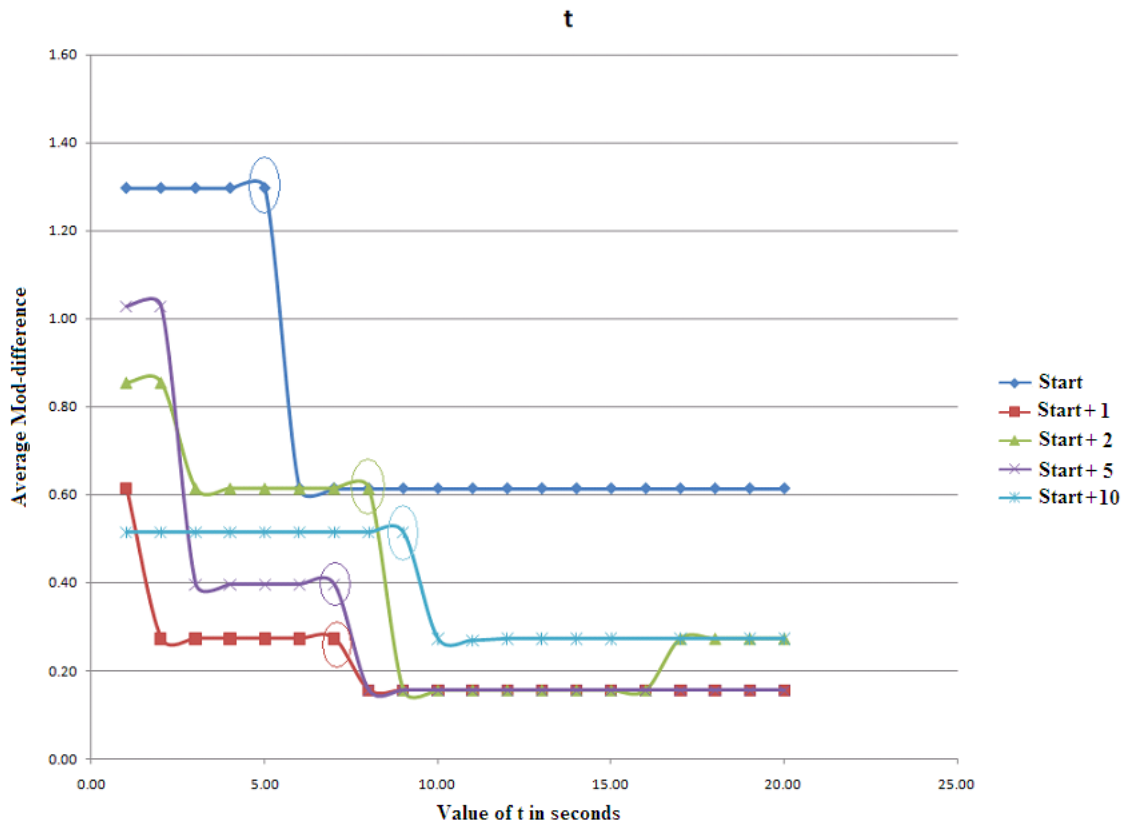


Figure 4.3: Average error (in mod-difference terms) for various  $t$  values

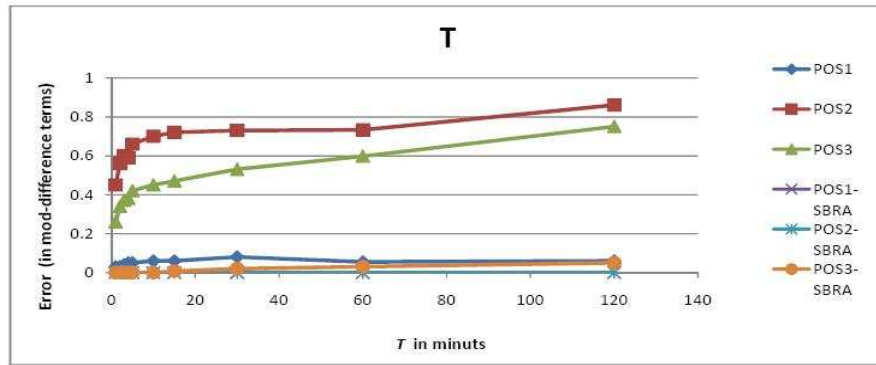


<b>t</b> <b>(in secs)</b>	<b>T=0 min</b>	<b>T=1 min</b>	<b>T=2 min</b>	<b>T=5 min</b>	<b>T=10 min</b>
<b>1</b>	1.30	0.61	0.85	1.03	0.51
<b>2</b>	1.30	0.27	0.85	1.03	0.51
<b>3</b>	1.30	0.27	0.61	0.40	0.51
<b>4</b>	1.30	0.27	0.61	0.40	0.51
<b>5</b>	1.30	0.27	0.61	0.40	0.51
<b>6</b>	0.61	0.27	0.61	0.40	0.51
<b>7</b>	0.61	0.27	0.61	0.40	0.51
<b>8</b>	0.61	0.16	0.61	0.16	0.51
<b>9</b>	0.61	0.16	0.16	0.16	0.51
<b>10</b>	0.61	0.16	0.16	0.16	0.51
<b>11</b>	0.61	0.16	0.16	0.16	0.27
<b>12</b>	0.61	0.16	0.16	0.16	0.61
<b>13</b>	0.61	0.16	0.16	0.16	0.27
<b>14</b>	0.61	0.16	0.16	0.16	0.27
<b>15</b>	0.61	0.16	0.16	0.16	0.27
<b>16</b>	0.61	0.16	0.16	0.16	0.61
<b>17</b>	0.61	0.16	0.27	0.16	0.27
<b>18</b>	0.61	0.16	0.27	0.16	0.61
<b>19</b>	0.61	0.16	0.27	0.16	0.27
<b>20</b>	0.61	0.16	0.27	0.16	0.27

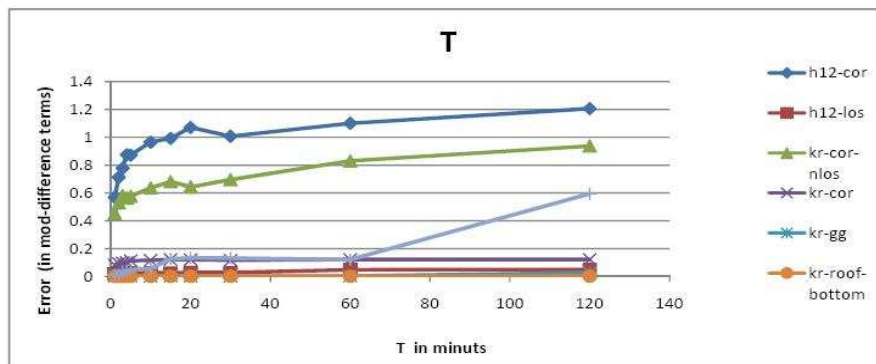
Table 4.1: Average error (in mod-difference terms) for various  $t$  values

With the  $t$  fixed at 10 seconds, we now go on to analyze the  $T$ . As described above we calculate the average error occurred for various  $T$  values.

The Figures 4.4(a) and 4.4(b) show the result of  $T$  analysis for various 802.11 and 802.15.4 locations respectively. We can observe that the average error over the 24 hr duration increases with the increase in  $T$  value as expected. But after  $T > 30$  mins the rate of increase in the error is very less in most of the cases, indicating that the  $T$  value can actually be taken as sufficiently large, without increasing the actual measurement error by much. So, we should determine  $T$  by looking at the network down time we intend to bear with during measurements. For example, given a network of size  $S$ , the total duration for single measurement would be  $S * t$ . Now, if we repeat measurement every  $T$  seconds, the total network downtime would be  $S * t / T$ . We know that the typical size of an LACN network can be equal to 10 nodes, so if we take the  $T$  value to be 2 hrs we would have a network downtime of 1.33 percent. Similarly if we take  $T$  as 3 hrs network downtime would be 0.30 percent. We now take these  $T$  and  $t$  values and try to design an automated mechanism for interference measurement strategy.



(a) 802.11



(b) 802.15.4

Figure 4.4: Average Error (in mod-difference terms) for various  $T$  values per different locations

## Chapter 5

# Putting It together: An Automated Interference mapping

In this chapter, we put together all the analysis we did so far to develop an automated system to generate the interference map.

### 5.1 Introduction

We have designed our system specifically for multi-hop TDMA based networks, especially for out-door mesh networks like FRACTEL . The important assumptions we made for this work are:

1. The network will have a central authority, which can control other nodes in the network and can bring the network down for measurements.
2. The central node is a computationally more capable node, and generates the interference map from the data sent by other nodes.
3. The network has time-synchronization; clocks on all nodes must be synchronized to a global clock.

For the purpose of measuring interference we take an active monitoring approach. Active monitoring allows us to stop the regular traffic and inject specific traffic into the network

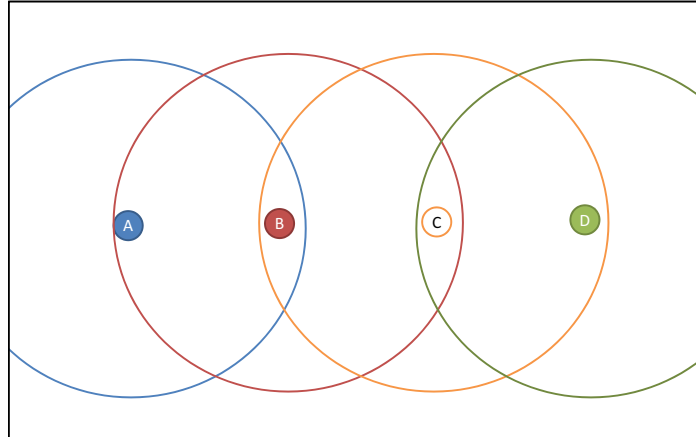


Figure 5.1: An example interference scenario

to study interference. We can control the transmission schedule at each node, along with the other network parameters like channel, transmission rate and size of the packet etc. As we have to perform controlled RSSI measurements for the purpose of interference estimation active monitoring is the best choice.

Our main objectives for the automated system are:

1. To perform regular controlled measurements at all the nodes according to the schedule given by the central node.
2. To generate the interference map, that provides complete information on inter-link interference among all the links in the network, at the central node.
3. To create the schedule of transmission for next interference measurements.

The interference map is a 3-dimensional matrix which divides each node into one of the three categories (described in Section 3.3) with respect to every link parents. For example, consider the simple network depicted in the Figure 5.1. It has four nodes A,B,C,D with each node in range only with its neighbor.

So, the interference map would be the following 3-dimensional matrix. Here, N represents that there is no communication link between the pair of nodes, X represents that the node is

<b>A</b>	A	B	C	D	<b>B</b>	A	B	C	D
A	X	X	X	X	A	X	X	N	N
B	X	X	3	N	B	X	X	X	X
C	X	1	X	3	C	N	X	X	N
D	X	N	3	X	D	N	X	1	X
<b>C</b>	A	B	C	D	<b>D</b>	A	B	C	D
A	X	1	X	N	A	X	3	N	X
B	3	X	X	N	B	3	X	1	X
C	X	X	X	X	C	N	3	X	X
D	N	N	X	X	D	X	X	X	X

Table 5.1: Interference Map

one of the ends of communication, hence no need to classify. The other nodes are classified as one among 1 - Interfering, 2- Variable and 3- Non interfering as described in Section 3.3.

Though this kind of interference matrix is very sparse, and can be reduced, this way of representing is easy to understand and ready to use in the sense that spatial reuse is possible among link pairs which are depicted as non interfering.

## 5.2 An automated measurement and spatial reuse map generation procedure

The aim of these measurements is to measure the RSSI values of every node in the network, at every other node. We know from the standard as well as [8] that in 802.11b, the interference range is greater than that of the transmission range (according to the standard for 802.11a these two ranges are same). This makes it difficult to detect interference because the packets which might not even be received might cause interference. For this purpose we do our RSSI measurement using a transmit power higher than the actual node transmit power. In fact we perform the measurement at the maximum transmit power. Also, we measure the transmission at minimum transmit rate. This is because of the fact that threshold for reception in 1Mbps links is much less than that of 11Mbps links. This has already been proved in [11]. We will also perform our measurements on a single pre-designated channel. We can later interpolate the RSSI values to the operating channel and calculate the interference. This is done by using the *receiver adjacent channel rejection* [3] techniques specified in the IEEE 802.11 draft.

Our automated system uses a client-server approach with central node acting as the server. The measurement schedule is determined at the sender and given to all other nodes. The generation of interference map is also done at the sender.

### 5.2.1 Active Measurement

#### Central Server:

- Central node creates a broadcast schedule (we discuss the creation of broadcast schedule in the next sub-section) that gives each node a *broadcast-time stamp*, which tells each node when exactly to broadcast. The schedule also gives the *start time* and the *end time* of the measurements so that the nodes will start listening to the other nodes' broadcasts.
- It then transmits this schedule to every node in the network.

#### Client:

- All the nodes in the network run a background daemon which is continuously listening for a schedule from the server.
- When the schedule is given by the central node, each node in the network broadcasts in turn according to its *broadcast-time*. They broadcast continuous stream of UDP packets of size 1400 bytes for a duration  $t$  (which we calculated to be 10 seconds in Section 4.3). They use maximum transmit power and minimum rate as discussed above.
- Every node, will listen from *start-time* to *end-time* (except when it is broadcasting) and summaries the RSSI information of every packet into a *RSSI matrix*. This *RSSI matrix* data structure is a two dimensional matrix that gives the count of the number of packets received per each node with a particular RSSI value.
- After a single cycle of measurements (after *end-time*), each of the nodes sends back its own *RSSI matrix* to the central node.

After data collection, the server creates interference map and schedule for next transmission, which is described in the following subsections. The whole procedure is again repeated after an interval of measurement time-period ( $T$ ).

### 5.2.2 Interference Map Generation

Once the measurements are complete the RSSI-matrix from various nodes is collected at the central node. The central node then uses this information to create the interference map. At first the RSSI information is modified according to the channel of operation.

The modified RSSI information is used to calculate the SIR values for each of the link pairs in the network. We classify each of the link-pairs into one of the three categories described in Section 3.3 and generate an interference map as shown in the example in Section 5.1.

### 5.2.3 Broadcast Schedule Generation

The above procedure of measurements require each node to broadcast independently for  $t$  (10 seconds). So the complexity of the measurement procedure would only be  $O(N)$ .  $N$  measurements are required for a network with  $N$  nodes. The total time taken now is equal to  $t * N$  seconds. We can still reduce this total time taken for measurement by scheduling broadcasts of non-conflicting nodes together.

The interference map thus generated can be used to generate the spatial reuse map, which can be used for TDMA scheduling, routing and channel assignment.

## Chapter 6

# Conclusion and Future work

### 6.1 Conclusion

In this work, we have developed a completely automated system for generating the spatial reuse map for 802.11b based TDMA networks. The system developed is based on actual RSSI measurements, and would take exactly  $N$  broadcast measurements for an  $N$ -node network to generate the interference map. One of the important aspects of this work is that we studied the system keeping in mind the typical RSSI variability of out-door wireless links. The work we did can be divided into two parts - interference estimation and time period analysis.

To develop the interference estimation strategy, we performed various measurements to study the relation between the measured RSSI values and the interference observed. We used the measured SIR distributions in combination with the SIR vs delivery probability curves to propose an interference estimation strategy. We then established that: though it is not possible to predict the exact delivery probability values in these kinds of settings, the general link behavior can be predicted. Finally, we developed a three way classification strategy so that it can be used for the purpose of generating interference map.

We then went on to do time period analysis to determine two important characteristics for automation: the measurement duration ( $t$ ), and measurement interval ( $T$ ). For this, we have analyzed long duration data from [8]. We also collected long duration data for 802.15.4 links. Through actual error evaluation of the long distance links, we found the practical value for the  $t$  to be 10 seconds. The  $T$ -value on the other hand can be judged according to the



required network up-time.

We finally developed an active measurement strategy to automatically perform  $O(N)$  measurements every  $T$ -time and generate interference map.

## 6.2 Future Work

There is a lot of scope for future work in this area. First among it would be integrating the above developed active measurements with passive monitoring, where the traffic in the network is monitored continuously to observe any kind of interlink interference. This can be done by separately creating a virtual interface in monitor mode. Using passive monitoring we can schedule measurements according to the error observed instead of a fixed cycle.

The work also needs to be tested in a real TDMA deployment. It would be interesting to evaluate how useful the interference information is in practice, for TDMA scheduling, or link channel selection. Also, the work only deals with 802.11b networks, and need to be extended for 802.11g and 802.11a.

# Bibliography

- [1] Digital Gangetic Plains, <http://www.cse.iitk.ac.in/users/braman/dgp.html>.
- [2] Djurslands International Institute of Rural Wireless Broadband, <http://diirwb.net/index.php?s=eu>.
- [3] IEEE Standard for Information Technology, Telecommunications and information exchange between systems, Local and metropolitan area networks - Specific requirements. Part 11: Wireless LAN Medium Access Control (MAC) and Physical Layer (PHY) Specifications.
- [4] MIT Roofnet, <http://pdos.csail.mit.edu/roofnet/doku.php>.
- [5] Daniel Aguayo, John Bicket, Sanjit Biswas, Glenn Judd, and Robert Morris. Link-level measurements from an 802.11b mesh network. In *Proc. of ACM SIGCOMM'2004 Conference*, Portland, Oregon, August 2004.
- [6] Maya Rodrig David Wetherall John Zahorjan Charles Reis, Ratul Mahajan. Measurement-based models of delivery and interference in static wireless networks. In *Conference on applications, technologies, architectures, and protocols for computer communications*, 2006.
- [7] Kameswari Chebrolu and Bhaskaran Raman. FRACTEL: a fresh perspective on (rural) mesh networks. In *CM SIGCOMM Workshop on Networked Systems for Developing Regions (NSDR'07)*, 2007.

- [8] Dattatraya Gokhale, Sayandeep Sen, Kameswari Chebrolu, and Bhaskaran Raman. On the Feasibility of the Link Abstraction in (Rural) Mesh Networks. In *IEEE INFOCOM*, Apr 2008.
- [9] Wonho Kim Daehyung Jo Taekyoung Kwon Yanghee Choi Jeongkeun Lee, Sung-Ju Lee. RSS-based Carrier Sensing and Interference Estimation in 802.11 Wireless Networks. In *Sensor, Mesh and Ad Hoc Communications and Networks, 2007. SECON '07.*, 2007.
- [10] Venkata N. Padmanabhan Lili Qiu Ananth Rao Brian Zill Jitendra Padhye, Sharad Agarwal. Estimation of Link Interference in Static Multi-hop Wireless Networks. In *ACM, Internet Measurement Conference*, 2005.
- [11] Bhaskaran Raman Kameshwari Chebrolu and Sayandeep Sen. Long Distance 802.11b: Performance Measurements and Experience. In *MOBICOM*, 2006.
- [12] Feng Wang Mi Kyung Han Ratul Mahajan Lili Qiu, Yin Zhang. A general model of wireless interference. In *ACM, International Conference on Mobile Computing and Networking*, 2007.
- [13] Dragos̃ Niculescu. Interference Map for 802.11 Networks. In *Internet Measurement Conference (IMC'07)*, 2007.
- [14] Bhaskaran Raman and Kameswari Chebrolu. Experiences in using wifi for rural internet in india. In *IEEE Communication. Magazine*, January 2007.
- [15] Y. Charlie Hu Saumitra M. Das, Dimitrios Koutsonikolas and Dimitrios Peroulis. Characterizing MultiWay Interference In Wireless Mesh Networks. In *International Conference on Mobile Computing and Networking (WiNTECH'06)*, 2006.
- [16] Sayandeep Sen and Bhaskaran Raman. Long Distance Wireless Mesh Network Planning: Problem Formulation and Solution. In *The 16th Annual Interntional World Wide Web Conference (WWW 2007)*, May 2007.